

Received December 28, 2021, accepted January 7, 2022, date of publication January 14, 2022, date of current version March 9, 2022.

Digital Object Identifier 10.1109/ACCESS.2022.3143541

Efficient Stochastic Model for Operational Availability Optimization of Cooling Tower Using Metaheuristic Algorithms

ASHISH KUMAR¹, MONIKA SAINI¹, NIVEDITA GUPTA¹,
DEEPAK SINWAR², (Member, IEEE), DILBAG SINGH³, (Member, IEEE),
MANJIT KAUR³, (Member, IEEE), AND HEUNG-NO LEE³, (Senior Member, IEEE)

¹Department of Mathematics and Statistics, Manipal University Jaipur, Dehmi Kalan, Jaipur, Rajasthan 303007, India

²Department of Computer and Communication Engineering, Manipal University Jaipur, Dehmi Kalan, Jaipur, Rajasthan 303007, India

³School of Electrical Engineering and Computer Science, Gwangju Institute of Science and Technology, Gwangju 61005, South Korea

Corresponding author: Heung-No Lee (heungno@gist.ac.kr)

This work was supported in part by the National Research Foundation of Korea (NRF) Grant funded by the Korean government (MSIP) (NRF-2021R1A2B5B03002118) and this research was supported by the Ministry of Science and ICT (MSIT), Korea, under the ITRC (Information Technology Research Center) support program (IITP-2021-0-01835) supervised by the IITP (Institute of Information & Communications Technology Planning & Evaluation).

ABSTRACT Metaheuristic algorithms are extensively utilized to find solutions and optimize complex industrial systems' performance. In this paper, metaheuristic algorithms are utilized to predict the optimum value of the operational availability of a cooling tower in a steam turbine power plant. These techniques have some flaws like poor convergence speed, being stuck in local optima, and premature convergence. For this purpose, a novel efficient stochastic model is proposed for a cooling tower that is configured with six subsystems. The Markovian birth-death process is utilized to develop the Chapman-Kolmogorov differential-difference equations. All the random variables are statically independent, and repairs are perfect. Failure rates are exponentially distributed, while repair rates follow the arbitrary distribution. Steady-state availability (SSA) of the system is derived concerning various failure and repair rates. The sensitivity analysis of SSA is also performed to identify the most critical component. Further, system availability is optimized using genetic algorithm (GA) and particle swarm optimization (PSO) because they are found to be more suitable for such types of problems. It is revealed that the PSO outperforms GA in predicting the availability of cooling towers used in steam turbine power plants.

INDEX TERMS Particle swarm optimization, genetic algorithm, cooling tower, availability, Markov modeling.

I. INTRODUCTION

In physics, energy is termed as the capability to do work and occurs in the form of nuclear, thermal, renewable, electrical, chemical, kinetic, and potential. Energy remains in practice to transfer from one body to another. It is classified according to its nature. The heat converts itself as thermal while work done becomes mechanical energy. But all these kinds are associated with motion. Electrical energy is termed electricity generated through the transformation of other energy sources. This transformation/conversion is done in power plants. These industrial entities generate electricity from coal,

The associate editor coordinating the review of this manuscript and approving it for publication was Kuo-Ching Ying.

steam, thermal, wind, tidal, and nuclear-using generators and transform mechanical energy into electrical energy and transfer it to the grid to use it into society and industries. Nuclear, thermal, solar, wind, and coal feed power plants are situated in various countries and dominated according to the availability of primary energy sources as fuel. Thermal power plants are mostly established plants in various countries. In thermal power plants, water is heated up to generate steam, and then at high pressure, it passes through the turbine. The turbine spin operates the generator, and motion started between the coil of wire and magnet available in the generator. This whole process resulted in electricity flow inception. Very high heat is generated during this process, and waste heat is rejected to the atmosphere with the help of heat

rejection devices, namely cooling towers. It uses the process of evaporation of water to remove the heat. Cooling towers are vast entities divided into several zones like rain zone, fill packing zone and spray zone. These systems are very complex, and the operation of such systems is very crucial. The failure causes complete power plant failure that causes a severe effect on societal and industrial production. Hence, it becomes necessary to handle cooling towers with high reliability.

The cooling tower and steam generators of power plants have been simulated using an artificial neural network [1]. A modified and improved version of the butterfly optimization algorithm utilized in combined cooling, heat, and power (CCHP) system operated by proton exchange membrane fuel cells (PEMFC) [2]. A systematic review of the optimization algorithms applying sustainability energy is presented in the literature [3]. A study on the performance management of solar thermal power plants has been carried out using multi-objective dynamic programming for optimization [4]. An optimal design using the Cuckoo search algorithm (CSA) was proposed for a solar-hybrid cogeneration system [5]. The results of the cuckoo search have been compared with a genetic algorithm using MATLAB toolbox and an effective time-saving procedure using simple parallel computing is the key finding of this study. A groundbreaking technology developed for geothermal and cooling cogeneration systems [6]. To improve the efficiency zeotropic mixtures have been used in subsystems. The thermodynamical and optimization characteristics of this system are also analyzed. Thermo-flow measures of the dry cooling system designed with only one tower in power plants have been investigated [7].

An experimental study has been carried out to investigate the efficiency of the wet cooling tower having diverse packing compaction using the artificial neural network and particle swarm optimization algorithm [8]. An analysis to reduce water intake for cooling towers used in thermal power plants as a pilot study [9]. Membrane capacitive deionization (MCDI) has been done in this study. A response surface methodology is developed through which optima process conditions of MCDI cooling tower can be determined given cost and efficiency. Supercritical combined gas-steam cycle systems analyzed technically as well as economic aspects [10]. Here, it is recommended that investments in adopting components of the steam part may be balanced from higher profit. The impact of the integration of hybrid thermal plants into energy complexes has been investigated [11]. A generalized methodology for the selection and calculation of technology schemes for mini plants has been utilized. The concept of Thermo-economic has been chosen for deciding the criteria for the best option of placing a mini thermal plant. Failure evaluation of power industry instruments done using probabilistic arguments [12]. It is concluded through experimental results that the proposed framework gain superiority over other typical data-based approaches. Several techniques like failure mode and effect analysis, reliability block

diagram, semi-Markov process, minimal cut set approach, and Markov birth-death process, exist in the literature for reliability evaluation of industrial systems with a certain set of assumptions [67]. But when failure and repair rate of components follow memoryless property and exponential distribution then the Markov birth-death process approach is recommended [79]–[81].

Nature-inspired algorithms (NIAs) are very efficient algorithms used to find solutions and optimize complex industrial systems' performance. NIA is a group of efficient methodologies derived from natural activities [13]. In the present study, NIAs have been used to predict the optimum value of the operational availability of a cooling tower in a steam turbine power plant. These techniques have some lacks like being stuck in local optima and slow convergence rate. For this purpose, an efficient stochastic model has been proposed for cooling towers configured with six subsystems. Markovian birth-death process has been utilized to develop the Chapman-Kolmogorov differential-difference equations. All the random variables are statistically independent, and repairs are perfect. Failure rates are exponentially distributed, while repair rates follow the arbitrary distribution. Steady-state availability of the system has been derived concerning various failure and repair rates. Further, system availability has been optimized using the Genetic Algorithm (GA) [50], [51] and Particle Swarm Optimization (PSO) [52]. The results will be shared with plant personnel. It is revealed the PSO outperforms GA in predicting the availability.

In short, the major contribution of this work is highlighted as follows:

- A novel efficient stochastic model is developed using the concept of cold standby redundancy for a cooling tower of Steam Turbine Power Plants.
- Availability and profit analysis of cooling towers are achieved by considering all failure rates as exponentially distributed while repair rates as arbitrary.
- Sensitivity analysis of availability function is carried out to identify the most critical component.
- Metaheuristic techniques namely Genetic Algorithm (GA) and Particle Swarm Optimization (PSO) are applied to obtain the optimum availability of the proposed model.
- Validation of obtained results is statistically investigated using Mann-Whitney U Test.

The remainder of this paper is organized as follows: Section 2 presents some work related to the work presented in this manuscript. Nomenclature, system description, and assumptions are provided in Section 3. Section 4 presents the stochastic modeling and sensitivity analysis of the cooling tower subsystem. Profit analysis is depicted in Section 5. Section 6 depicts materials and methods viz. reliability measures, Markov process, simulation environment, and optimization strategies. Numeric results and discussions are presented in Section 7. Finally, Section 8 presents the concluding remarks with some future directions.

II. RELATED WORK

Many studies have been done by researchers related to steam turbine power plants and their subsystems. Reliability aspects of combined cycle power plants (CCPP) were studied through mathematical modeling and availability analysis because generators play a critical role in the operation of CCPP and steam turbine power plants [15]. Operational availability investigation of these systems has been done using the Markovian approach [14]. Advanced data mining techniques supported by data like support vector regression and data reconciliation have been used in air-cooling condensers of thermal power plants [16]. The applicability of dry cooling towers as condensers has been observed in geothermal power plants [17]. A reliability-based approach has been proposed for maintenance in combined cycle power plants based on identifying the most critical component of it [18]. Some amendments in the VGB guidelines suggested improving the design for manufacturing cooling towers in power plants [19]. The effect of climate change on cooling towers' performance was investigated to optimize technical, economic, and design perspectives [20]. Performance evaluation of thermal power plants to improve accuracy and reliability model-based data reconciliation techniques has been used [21]. A systematic review was done to observe the performance of natural draft dry cooling towers by using inlet air spray [22]. The use of cooling towers in chimneys and solar power plants is discussed in [23]. The technical aspects of cooling towers associated with river basins have been appended in [24]. A new design of the hybrid cooling system for large-scale steam turbine power plant generators was developed to assess the performance [25]. The water flow in the power plant's cooling towers also shows a significant effect, and a numerical investigation has been done in this direction [26], [27]. An investigation was made to assess thermal power plants' sustainability in low water areas using cooling towers [28]. Fault tree analysis and system reliability evaluation have been done for combined cycle power plants [29]. The performance assessment and optimization of spray cooling system design in solar power plants is studied in [30]. Machine learning techniques are frequently used to optimize evaporation-based cooling towers, and performance is optimized using particle swarm optimization [31]. A novel model exists in the literature to understand water use in power plants [32]–[36]. A prediction model for performance and cost analysis in hybrid cooling towers in power plants has been developed [33]. The stochastic Petri nets technique is utilized to develop efficient and optimized maintenance strategies for a coal-fired power plant [34]. The mathematical model for efficiency prediction of thermal plants' cooling towers was discussed and extended it up to three towers [35]. A new methodology for the reliability evaluation of thermal power plants is proposed under different assumptions [37]. Energy-saving benefits and economic evaluation of cooling towers using fuel gas are analyzed [38]. Variable ambient conditions that impact the cooling system of power plants are investigated using mathematical modeling [39].

During the last few years, reliability analysis and optimization of thermal plants have attracted researchers. A Multicriteria decision-making model for optimization of operational routes in thermal power plants has been developed [40]. A study for reliability improvement of power systems using the idea of transmission line switching has been conducted with ac power flows [41]. The reliability evaluation of power systems using power outage modeling is carried out by the researcher [42]. The combination of Markov and matrix methods is extensively used in reliability assessment [43]. The reliability evaluation of wind power plants also attracted researchers [44], [45]. Recently, several advanced metaheuristics approaches were developed for the performance optimization of industrial systems [46]–[48], [67]. Some popular optimization algorithms namely Chimp, dynamic Levy flight chimp, and weighted Chimp optimization algorithms are proposed for the optimization of industrial systems [68], [69], [71]. For sonar dataset classification some improved migration models based on biogeography-based optimization has been proposed using neural network [70]. Recently, a new binary metaheuristic algorithm Binary Chimp Optimization Algorithm (BChOA) is developed for solving the optimization problem [72]. Various algorithms like chaotic fractal walk trainer, whale trainer, modified grey wolf optimizer, and fuzzy grasshopper optimizer are proposed for sonar data analysis [73]. Deep learning models [74]–[78] have been extensively utilized to solve many optimization problems too. But due to non-availability of the required data, we have used metaheuristic techniques only. Sensitivity analysis of the algorithms and parameter initializations in metaheuristics is also important and has wide applicability in optimization algorithms [79]. The literature review observed that several studies were conducted on performance analysis of steam turbine power plants. But reliability aspects of steam turbine power plants and their components like cooling towers are still not explored extensively. The optimization of reliability measures of cooling towers and steam turbine power plants were not discussed yet. Therefore, in this paper, to optimize the availability of cooling towers, nature-inspired algorithms like genetic algorithms and particle swarm optimization are used.

III. PRELIMINARIES

A. NOMENCLATURE

Following notations are utilized to develop the mathematical model of the cooling tower:



B. SYSTEM DESCRIPTION

A concise depiction of a cooling tower in a steam turbine power plant has been given in this part. Cooling tower mainly comprises seven parts: hydro turbine, pressure-driven valves, water splash framework, programmed deaerator valves, cooling water siphon, engine valves, and standpipe. All segments are organized in a series arrangement. The concept of cold standby redundancy at the component level is adopted. All the

TABLE 1. Notation of various system states, failure rates, and repair rates.

Sub-system	Operative Mode	Failed Mode	Failure rate (ϑ_i)	Repair rate $\sigma_i(y)$
Hydro Turbine	S	s	ϑ_1	$\sigma_1(y)$
Hydraulic valve	T	t	ϑ_2	$\sigma_2(y)$
Water spray system	U	u	ϑ_3	$\sigma_3(y)$
Automatic deaerator valves	V, V1	V	ϑ_4	$\sigma_4(y)$
Cooling water pump	W	w	ϑ_5	$\sigma_5(y)$
Motor valve	X	x	ϑ_6	$\sigma_6(y)$
Standpipe	Y	y	ϑ_7	$\sigma_7(y)$

N_i ($i = 0, 1, 2, \dots, 7$): Probability that system is in i^{th} state
 $N_0(t)$: At time t system at 0 state

 Operative State
 Failed State

time-dependent random variables associated with failure and repair rates of components are statistically independent. The failed component after the repair was performed as a new one. A sufficient repair facility is available with the system.

The visual portrayal of segments is shown in Figure 1. The working of different components of the cooling tower subsystem are briefed as under:

- 1) Hydro turbine: It comprises one unit of a hydro turbine. This current unit’s disappointment causes total framework disappointment as it is associated with different units in series.
- 2) Hydraulic valves: It comprises one bunch of Hydraulic valves. This present unit’s failure causes total framework failure as it is associated with different units in series.

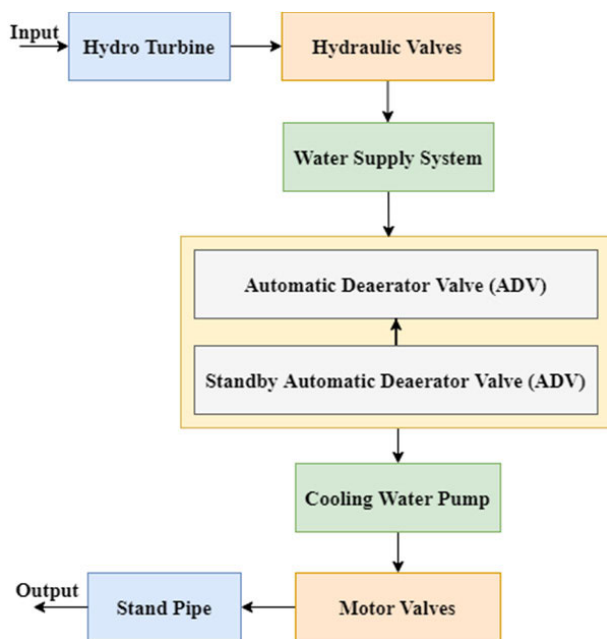


FIGURE 1. Configuration diagram of Cooling tower subsystem.

- 3) Water supply framework: It comprises one unit of water splash framework. This current unit’s failure causes total framework failure as it is associated with different units in series.
- 4) Programmed deaerator valves: It comprises two arrangements of programmed de-aerator valves; one is employable, and the other is on standby. The disappointing pace of both units is the same, and the disappointment of the two units keeps an eye on framework disappointment.
- 5) Cooling water siphon: It comprises one unit of Cooling Water Pump. This present unit’s failure causes total framework failure as it is associated with different units in series.
- 6) Engine valves: It comprises one bunch of engine valves. This current unit’s failure causes total framework failure as it is associated with different units in series.
- 7) Standpipe: It comprises one bunch of engine valves. This present unit’s failure causes total framework failure as it is associated with different units in series.

C. ASSUMPTIONS

For the development of the model, several assumptions are incorporated as follows:

- 1) The failure rate of subsystems follows an exponential distribution, whereas repair rates are arbitrarily distributed (as per Table 1).
- 2) Random variables are independent and identical to each other.
- 3) Case of concurrent failures not considered in model development.
- 4) Perfect repairs and switch-over devices.
- 5) Availability of sufficient repair facilities in the plant.

IV. STOCHASTIC MODELING AND SENSITIVITY ANALYSIS OF COOLING TOWER

By using simple probabilistic arguments and the Markov birth-death process, a novel stochastic model is developed as shown in Figure 2. Analytical solution of the proposed stochastic model is obtained using the supplementary variable technique. The differential-difference equations are as follows:

$$\begin{aligned}
 N_0(t + \Delta t) &= (1 - \vartheta_1 \Delta t - \vartheta_2 \Delta t - \vartheta_3 \Delta t - \vartheta_4 \Delta t - \vartheta_5 \Delta t \\
 &\quad - \vartheta_6 \Delta t - \vartheta_7 \Delta t) N_0(t) + \int_0^\infty \sigma_1(y) N_1(y, t) \Delta t dy \\
 &\quad + \int_0^\infty \sigma_2(y) N_2(y, t) \Delta t dy \\
 &\quad + \int_0^\infty \sigma_3(y) N_3(y, t) \Delta t dy + \int_0^\infty \sigma_4(y) N_4(y, t) \Delta t dy \\
 &\quad + \int_0^\infty \sigma_5(y) N_5(y, t) \Delta t dy + \int_0^\infty \sigma_6(y) N_6(y, t) \Delta t dy \\
 &\quad + \int_0^\infty \sigma_7(y) N_7(y, t) \Delta t dy
 \end{aligned} \tag{1}$$

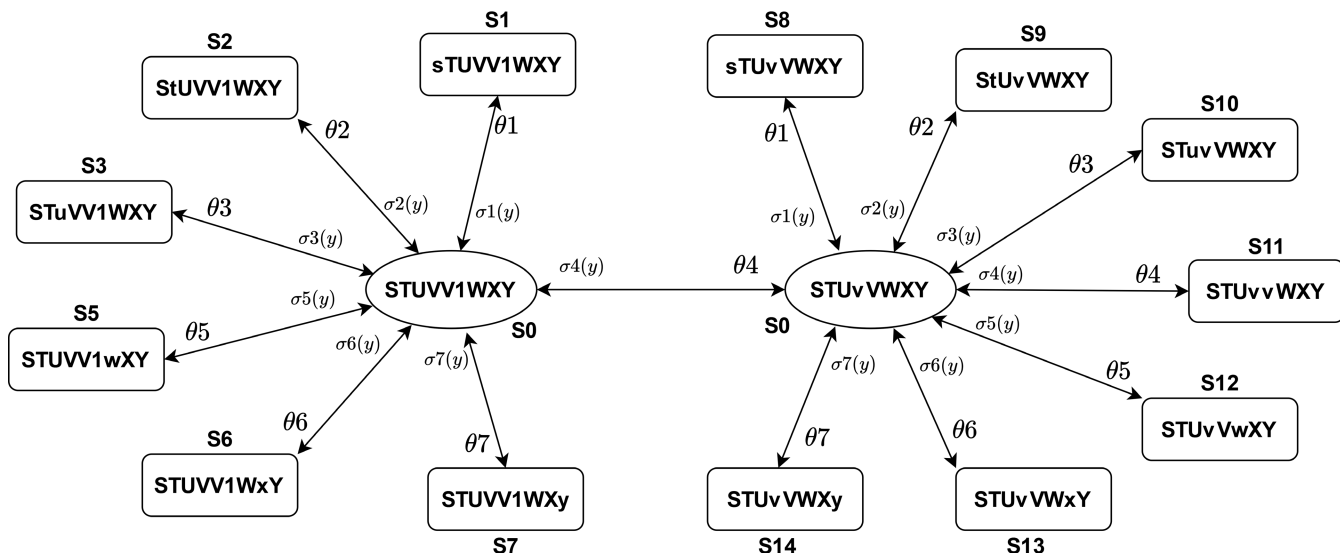


FIGURE 2. State transition diagram of a generator in steam turbine power plant.

Dividing both the sides of Eq. (1) by Δt , we get

$$\begin{aligned} & \frac{N_o(t + \Delta t) - N_o(t)}{\Delta t} \\ &= (-\vartheta_1 - \vartheta_2 - \vartheta_3 - \vartheta_4 - \vartheta_5 - \vartheta_6 \\ & \quad - \vartheta_7) N_o(t) + \int_0^\infty \sigma_1(y) N_1(y, t) dy \\ & \quad + \int_0^\infty \sigma_2(y) N_2(y, t) dy \\ & \quad + \int_0^\infty \sigma_3(y) N_3(y, t) dy + \int_0^\infty \sigma_4(y) N_4(y, t) dy \\ & \quad + \int_0^\infty \sigma_5(y) N_5(y, t) dy + \int_0^\infty \sigma_6(y) N_6(y, t) dy \\ & \quad + \int_0^\infty \sigma_7(y) N_7(y, t) dy \end{aligned} \tag{2}$$

As $\Delta t \rightarrow 0$ on Eq. (2), we obtain Eq. (3) as follows:

$$\begin{aligned} & \lim_{\Delta t \rightarrow 0} \frac{N_o(t + \Delta t) - N_o(t)}{\Delta t} \\ &= (-\vartheta_1 - \vartheta_2 - \vartheta_3 - \vartheta_4 - \vartheta_5 - \vartheta_6 \\ & \quad - \vartheta_7) N_o(t) + \int_0^\infty \sigma_1(y) N_1(y, t) dy \\ & \quad + \int_0^\infty \sigma_2(y) N_2(y, t) dy + \int_0^\infty \sigma_3(y) N_3(y, t) dy \\ & \quad + \int_0^\infty \sigma_4(y) N_4(y, t) dy + \int_0^\infty \sigma_5(y) N_5(y, t) dy \\ & \quad + \int_0^\infty \sigma_6(y) N_6(y, t) dy + \int_0^\infty \sigma_7(y) N_7(y, t) dy \tag{3} \\ &\Rightarrow \frac{dN_o}{dt} + (\vartheta_1 + \vartheta_2 + \vartheta_3 + \vartheta_4 + \vartheta_5 + \vartheta_6 + \vartheta_7) N_o(t) \\ &= \int_0^\infty \sigma_1(y) N_1(y, t) dy + \int_0^\infty \sigma_2(y) N_2(y, t) dy \\ & \quad + \int_0^\infty \sigma_3(y) N_3(y, t) dy + \int_0^\infty \sigma_4(y) N_4(y, t) dy \end{aligned}$$

$$\begin{aligned} & + \int_0^\infty \sigma_5(y) N_5(y, t) dy + \int_0^\infty \sigma_6(y) N_6(y, t) dy \\ & + \int_0^\infty \sigma_7(y) N_7(y, t) dy \end{aligned} \tag{4}$$

The Eq. (4) can be expressed in abbreviated form using summation and represented as Eq. (5).

$$\Rightarrow \frac{dN_o}{dt} + \sum_{i=1}^7 \vartheta_i N_o(t) = \sum_{i=1}^7 \int_0^\infty \sigma_i(y) N_i(y, t) dy \tag{5}$$

$$\Rightarrow \left(\frac{d}{dt} + u_0\right) N_o(t) = f_0 \tag{6}$$

Here, $u_0 = \sum_{i=1}^7 \vartheta_i$ & $f_0 = \sum_{i=1}^7 \int_0^\infty \sigma_i(y) N_i(y, t) dy$
Similarly,

$$N_1(y + \Delta y, t + \Delta t) = \vartheta_1 \Delta t N_o(t) + (1 - \sigma_1(1) \Delta y) N_1(y, t) \tag{7}$$

Differentiate Eq. (7) by considering y and t partially as:

$$\begin{aligned} & \left(\frac{\partial}{\partial y} + \frac{\partial}{\partial t} + \sigma_i(1)\right) N_i(y, t) \\ &= \vartheta_i N_o(t) \quad \forall i = 1, 2, 3, 5, 6, 7 \end{aligned} \tag{8}$$

$$\begin{aligned} & N_4(y + \Delta y, t + \Delta t) \\ &= (1 - \vartheta_1 \Delta t - \vartheta_2 \Delta t - \vartheta_3 \Delta t \\ & \quad - \vartheta_4 \Delta t - \vartheta_5 \Delta t - \vartheta_6 \Delta t - \vartheta_7 \Delta t) (1 - \sigma_4(1) \Delta t) N_4(y, t) \\ & \quad + \vartheta_4 \Delta t N_o(t) + \sigma_1(1) \Delta y N_8(y, t) + \sigma_2(1) \Delta y N_9(y, t) \\ & \quad + \sigma_3(1) \Delta y N_{10}(y, t) + \sigma_4(y) \Delta y N_{11}(y, t) + \sigma_5(1) \Delta y \\ & \quad \times N_{12}(y, t) + \sigma_6(1) \Delta y N_{13}(y, t) \\ & \quad + \sigma_7(1) \Delta y N_{14}(y, t) \end{aligned} \tag{9}$$

Differentiate Eq. (9) by considering y and t partially as:

$$\begin{aligned} \Rightarrow \left(\frac{\partial}{\partial y} + \frac{\partial}{\partial t} + \beta_4(1) + \sum_{i=1}^7 \vartheta_i \right) N_4(y, t) &= \vartheta_4 N_0(t) \\ &+ \beta_1(1) N_8(y, t) + \beta_2(1) N_9(y, t) \\ &+ \beta_3(1) N_{10}(y, t) + \beta_4(1) N_{11}(y, t) + \beta_5(1) N_{12}(y, t) \\ &+ \beta_6(1) N_{13}(y, t) + \beta_7(1) N_{14}(y, t) \end{aligned} \quad (10)$$

Eq. (11) is derived using Eq. (9-10) as:

$$\Rightarrow \left(\frac{\partial}{\partial y} + \frac{\partial}{\partial t} + \beta_4(1) + u_0 \right) N_4(y, t) = f_1(y, t) \quad (11)$$

Here,

$$\begin{aligned} f_1(y, t) &= \beta_1(y) N_8(y, t) + \beta_2(y) N_9(y, t) \\ &+ \beta_3(y) N_{10}(y, t) \\ &+ \beta_4(y) N_{11}(y, t) + \beta_5(y) N_{12}(y, t) + \beta_6(y) N_{13}(y, t) \\ &+ \beta_7(y) N_{14}(y, t) \end{aligned}$$

Similarly,

$$\begin{aligned} N_{7+j}(y + \Delta y, t + \Delta t) &= \vartheta_j \Delta t N_4(y, t) + (1 - \sigma_j(y) \Delta y) N_{7+j}(y, t) \\ \forall j &= 1, 2, \dots, 7 \end{aligned} \quad (12)$$

Differentiate Eq. (12) with respect to y and t partially as: get

$$\left(\frac{\partial}{\partial y} + \frac{\partial}{\partial t} + \sigma_j(y) \right) N_{7+j}(y, t) = \vartheta_j N_4(y, t) \quad \forall j = 1, 2, \dots, 7 \quad (13)$$

The boundary conditions are given as

$$\left\{ \begin{aligned} N_1(0, t) &= \vartheta_1 N_0(t) & N_2(0, t) &= \vartheta_2 N_0(t) \\ N_3(0, t) &= \vartheta_3 N_0(t) & N_4(0, t) &= \vartheta_4 N_0(t) \\ N_5(0, t) &= \vartheta_5 N_0(t) & N_6(0, t) &= \vartheta_6 N_0(t) \\ N_7(0, t) &= \vartheta_7 N_0(t) & N_8(0, t) &= \vartheta_1 N_4(t) \\ N_9(0, t) &= \vartheta_2 N_4(t) & N_{10}(0, t) &= \vartheta_3 N_4(t) \\ N_{11}(0, t) &= \vartheta_4 N_4(t) & N_{12}(0, t) &= \vartheta_5 N_4(t) \\ N_{13}(0, t) &= \vartheta_6 N_4(t) & N_{14}(0, t) &= \vartheta_7 N_4(t) \end{aligned} \right\} \quad (14)$$

and initial conditions are given as

$$N_i(t = 0) = \begin{cases} 1, & \text{if } i = 0 \\ 0, & \text{if } i = 1 \text{ to } 14 \end{cases} \quad (15)$$

Eqs. (6-13), boundary (14) and initial (15) conditions constitute a set of Chapman-Kolmogorov differential-difference [67]. In particular, to show the importance of results based on the availability of the system and profit analysis, we assume repair rates to follow an exponential distribution. Therefore, the boundary and initial conditions can be redefined as follows:

$$\begin{aligned} \left(\frac{d}{dt} + u_0 \right) N_o(t) &= \sigma_1 N_1(t) + \sigma_2 N_2(t) + \sigma_3 N_3(t) \\ &+ \sigma_4 N_4(t) + \sigma_5 N_5(t) + \sigma_6 N_6(t) \\ &+ \sigma_7 N_7(t) \end{aligned} \quad (16)$$

$$\left(\frac{d}{dt} + \sigma_i \right) N_i(t) = \vartheta_i N_0(t) \quad \forall i = 1, 2, 3, 5, 6, 7 \quad (17)$$

$$\begin{aligned} \left(\frac{d}{dt} + u_0 + \sigma_4 \right) N_4(t) &= \vartheta_4 N_0(t) + \sigma_1 N_8(t) + \sigma_2 N_9(t) \\ &+ \sigma_3 N_{10}(t) + \sigma_4 N_{11}(t) + \sigma_5 N_{12}(t) \\ &+ \sigma_6 N_{13}(t) + \sigma_7 N_{14}(t) \end{aligned} \quad (18)$$

$$\frac{d}{dt} + \sigma_j N_{7+j}(t) = \vartheta_j N_4(t) \quad \forall j = 1, 2, \dots, 7 \quad (19)$$

The steady-state probabilities and long-time availability of the system can be evaluated by using $\frac{d}{dt} = 0$ as $t \rightarrow \infty, N_i(t) = N_i$ in Eqs. (16-18) and initial conditions (15), we get

$$\left\{ \begin{aligned} \sigma_1 N_8 &= \vartheta_1 N_4 & \sigma_2 N_9 &= \vartheta_2 N_4 \\ \sigma_3 N_{10} &= \vartheta_3 N_4 & \sigma_4 N_{11} &= \vartheta_4 N_4 \\ \sigma_5 N_{12} &= \vartheta_5 N_4 & \sigma_6 N_{13} &= \vartheta_6 N_4 \\ \sigma_7 N_{14} &= \vartheta_7 N_4 & N_j &= \frac{\vartheta_i}{\sigma_i} N_4 \\ & & \text{where } i &= 1, 2, 3, 4, 5, 6, 7; \\ & & j &= 8, 9, 10, 11, 12, 13, 14 \\ \sigma_1 N_1 &= \vartheta_1 N_0 & \sigma_2 N_2 &= \vartheta_2 N_0 \\ \sigma_3 N_3 &= \vartheta_3 N_0 & \sigma_5 N_5 &= \vartheta_5 N_0 \\ \sigma_6 N_6 &= \vartheta_6 N_0 & \sigma_7 N_7 &= \vartheta_7 N_0 \\ N_0 N_j &= \frac{\vartheta_j}{\sigma_j} N_0 \\ & & \text{where } j &= 1, 2, 3, 5, 6, 7 \end{aligned} \right\} \quad (20)$$

From Eq. (20), the probability of states S_1 to S_{14} in terms of N_0 can be computed as:

$$\left\{ \begin{aligned} N_1 &= \frac{\vartheta_1}{\sigma_1} N_0 & N_2 &= \frac{\vartheta_2}{\sigma_2} N_0 \\ N_3 &= \frac{\vartheta_3}{\sigma_3} N_0 & N_4 &= \frac{\vartheta_4}{\sigma_4} N_0 \\ N_5 &= \frac{\vartheta_5}{\sigma_5} N_0 & N_6 &= \frac{\vartheta_6}{\sigma_6} N_0 \\ N_7 &= \frac{\vartheta_7}{\sigma_7} N_0 & N_8 &= \frac{\vartheta_1}{\sigma_1} N_4 = \frac{\vartheta_1 \vartheta_4}{\sigma_1 \sigma_4} N_0 \\ N_9 &= \frac{\vartheta_2 \vartheta_4}{\sigma_2 \sigma_4} N_0 & N_{10} &= \frac{\vartheta_3 \vartheta_4}{\sigma_3 \sigma_4} N_0 \\ N_{11} &= \frac{\vartheta_4^2}{\sigma_4^2} N_0 & N_{12} &= \frac{\vartheta_5 \vartheta_4}{\sigma_5 \sigma_4} N_0 \\ N_{13} &= \frac{\vartheta_4 \vartheta_6}{\sigma_4 \sigma_6} N_0 & N_{14} &= \frac{\vartheta_4 \vartheta_7}{\sigma_4 \sigma_7} N_0 \end{aligned} \right\} \quad (21)$$

Using normalizing condition $\sum_{i=0}^{14} N_i = 1$ and expressions given in Eq. (21), the following expression obtained:

$$\begin{aligned} \Rightarrow N_0 &= \left[1 + \frac{\vartheta_1}{\sigma_1} + \frac{\vartheta_2}{\sigma_2} + \frac{\vartheta_3}{\sigma_3} + \frac{\vartheta_4}{\sigma_4} + \frac{\vartheta_5}{\sigma_5} + \frac{\vartheta_6}{\sigma_6} + \frac{\vartheta_7}{\sigma_7} \right. \\ &+ \frac{\vartheta_1 \vartheta_4}{\sigma_1 \sigma_4} + \frac{\vartheta_2 \vartheta_4}{\sigma_2 \sigma_4} + \frac{\vartheta_3 \vartheta_4}{\sigma_3 \sigma_4} + \frac{\vartheta_4^2}{\sigma_4^2} + \frac{\vartheta_4 \vartheta_5}{\sigma_4 \sigma_5} + \frac{\vartheta_4 \vartheta_6}{\sigma_4 \sigma_6} \\ &\left. + \frac{\vartheta_4 \vartheta_7}{\sigma_4 \sigma_7} \right]^{-1} \end{aligned} \quad (22)$$

$$\begin{aligned} \Rightarrow N_0 &= \left[1 + \left(1 + \frac{\vartheta_4}{\sigma_4} \right) \left(\frac{\vartheta_1}{\sigma_1} + \frac{\vartheta_2}{\sigma_2} + \frac{\vartheta_3}{\sigma_3} + \frac{\vartheta_4}{\sigma_4} + \frac{\vartheta_5}{\sigma_5} \right. \right. \\ &\left. \left. + \frac{\vartheta_6}{\sigma_6} + \frac{\vartheta_7}{\sigma_7} \right) \right]^{-1} \end{aligned} \quad (23)$$

The steady-state availability of the system has been obtained using Eqs. (22-23) as follows:

$$A_v = N_0 + N_4 \Rightarrow A_v = N_0 + \frac{\vartheta_4}{\sigma_4} N_0 \Rightarrow A_v = \left(1 + \frac{\vartheta_4}{\sigma_4}\right) N_0 \tag{24}$$

As the availability of a cooling tower is crucial for the operation of STPP, its sensitivity analysis becomes necessary with respect to various failure rates [79]–[81]. Sensitivity is termed as the rate of change in availability and defined as the partial derivate of availability (24) with respect to θ_i . The partial derivatives are shown in Eqs. (25–31) and results of sensitivity analysis are presented in Table 13.

V. PROFIT ANALYSIS

Let K_1 be the total revenue per unit uptime of the system and K_2 be the total repair cost then profit incurred to the system model in steady-state is obtained as:

$$Profit = K_1 A_v - K_2 \tag{32}$$

The value of profit function after considering the arbitrary values for $K1 = 3500$ and $K2 = 500$ is defined in Eq. (33) as

follows:

$$Profit = [3500\left(1 + \frac{\vartheta_4}{\sigma_4}\right)N_0] - 500 \tag{33}$$

VI. MATERIALS AND METHODS

A. RELIABILITY MEASURES

1) RELIABILITY

It is the probability that the system performs its intended function under stated operating conditions without any failures. It ranges from 1 to 0.

2) AVAILABILITY

It is a kind of probability states that a system is available for utilization as and when required. It ranges from 0 to 1. At time $t = 0$, availability is 1, and at infinity, its value is 0. It is defined as the ratio of uptime and total life duration [67].

B. MARKOV PROCESS

It is a well-known stochastic process (developed by A.A. Markov) that is widely used in reliability and queuing theory. It states that the behavior of future states depends on the present conditions and is independent of the past [79]–[81].

$$\frac{\partial A}{\partial \theta_1} = \frac{-\frac{1}{\sigma_1} \left\{1 + \frac{\theta_4}{\sigma_4}\right\}^2}{\left\{1 + \left(1 + \frac{\theta_4}{\sigma_4}\right) \left(\frac{\theta_1}{\sigma_1} + \frac{\theta_2}{\sigma_2} + \frac{\theta_3}{\sigma_3} + \frac{\theta_4}{\sigma_4} + \frac{\theta_5}{\sigma_5} + \frac{\theta_6}{\sigma_6} + \frac{\theta_7}{\sigma_7}\right)\right\}^2} \tag{25}$$

$$\frac{\partial A}{\partial \theta_2} = \frac{-\frac{1}{\sigma_2} \left\{1 + \frac{\theta_4}{\sigma_4}\right\}^2}{\left\{1 + \left(1 + \frac{\theta_4}{\sigma_4}\right) \left(\frac{\theta_1}{\sigma_1} + \frac{\theta_2}{\sigma_2} + \frac{\theta_3}{\sigma_3} + \frac{\theta_4}{\sigma_4} + \frac{\theta_5}{\sigma_5} + \frac{\theta_6}{\sigma_6} + \frac{\theta_7}{\sigma_7}\right)\right\}^2} \tag{26}$$

$$\frac{\partial A}{\partial \theta_3} = \frac{-\frac{1}{\sigma_3} \left\{1 + \frac{\theta_4}{\sigma_4}\right\}^2}{\left\{1 + \left(1 + \frac{\theta_4}{\sigma_4}\right) \left(\frac{\theta_1}{\sigma_1} + \frac{\theta_2}{\sigma_2} + \frac{\theta_3}{\sigma_3} + \frac{\theta_4}{\sigma_4} + \frac{\theta_5}{\sigma_5} + \frac{\theta_6}{\sigma_6} + \frac{\theta_7}{\sigma_7}\right)\right\}^2} \tag{27}$$

$$\begin{aligned} \frac{\partial A}{\partial \theta_4} &= \left\{1 + \left(1 + \frac{\theta_4}{\sigma_4}\right) \left(\frac{\theta_1}{\sigma_1} + \frac{\theta_2}{\sigma_2} + \frac{\theta_3}{\sigma_3} + \frac{\theta_4}{\sigma_4} + \frac{\theta_5}{\sigma_5} + \frac{\theta_6}{\sigma_6} + \frac{\theta_7}{\sigma_7}\right)\right\} \frac{1}{\sigma_4} - \frac{1}{\sigma_4} \left(1 + \frac{\theta_4}{\sigma_4}\right) \\ &\times \left\{\left(1 + \frac{\theta_4}{\sigma_4}\right) + \left(\frac{\theta_1}{\sigma_1} + \frac{\theta_2}{\sigma_2} + \frac{\theta_3}{\sigma_3} + \frac{\theta_4}{\sigma_4} + \frac{\theta_5}{\sigma_5} + \frac{\theta_6}{\sigma_6} + \frac{\theta_7}{\sigma_7}\right)\right\} \\ &/ \left\{1 + \left(1 + \frac{\theta_4}{\sigma_4}\right) \left(\frac{\theta_1}{\sigma_1} + \frac{\theta_2}{\sigma_2} + \frac{\theta_3}{\sigma_3} + \frac{\theta_4}{\sigma_4} + \frac{\theta_5}{\sigma_5} + \frac{\theta_6}{\sigma_6} + \frac{\theta_7}{\sigma_7}\right)\right\}^2 \end{aligned} \tag{28}$$

$$\frac{\partial A}{\partial \theta_5} = \frac{-\frac{1}{\sigma_5} \left\{1 + \frac{\theta_4}{\sigma_4}\right\}^2}{\left\{1 + \left(1 + \frac{\theta_4}{\sigma_4}\right) \left(\frac{\theta_1}{\sigma_1} + \frac{\theta_2}{\sigma_2} + \frac{\theta_3}{\sigma_3} + \frac{\theta_4}{\sigma_4} + \frac{\theta_5}{\sigma_5} + \frac{\theta_6}{\sigma_6} + \frac{\theta_7}{\sigma_7}\right)\right\}^2} \tag{29}$$

$$\frac{\partial A}{\partial \theta_6} = \frac{-\frac{1}{\sigma_6} \left\{1 + \frac{\theta_4}{\sigma_4}\right\}^2}{\left\{1 + \left(1 + \frac{\theta_4}{\sigma_4}\right) \left(\frac{\theta_1}{\sigma_1} + \frac{\theta_2}{\sigma_2} + \frac{\theta_3}{\sigma_3} + \frac{\theta_4}{\sigma_4} + \frac{\theta_5}{\sigma_5} + \frac{\theta_6}{\sigma_6} + \frac{\theta_7}{\sigma_7}\right)\right\}^2} \tag{30}$$

$$\frac{\partial A}{\partial \theta_7} = \frac{-\frac{1}{\sigma_7} \left\{1 + \frac{\theta_4}{\sigma_4}\right\}^2}{\left\{1 + \left(1 + \frac{\theta_4}{\sigma_4}\right) \left(\frac{\theta_1}{\sigma_1} + \frac{\theta_2}{\sigma_2} + \frac{\theta_3}{\sigma_3} + \frac{\theta_4}{\sigma_4} + \frac{\theta_5}{\sigma_5} + \frac{\theta_6}{\sigma_6} + \frac{\theta_7}{\sigma_7}\right)\right\}^2} \tag{31}$$

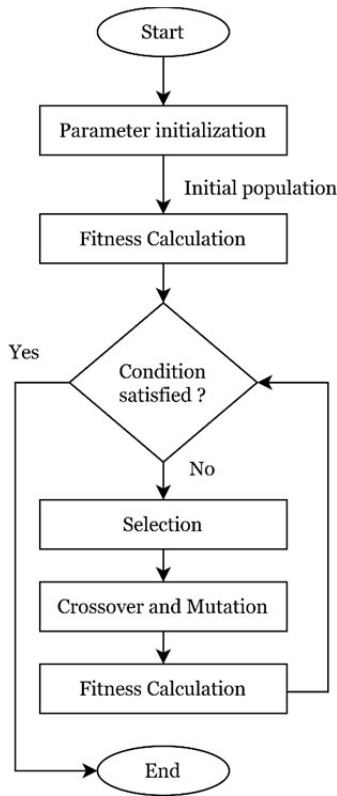


FIGURE 3. Flowchart of genetic algorithm.

A process of continuous time discrete space is utilized in the reliability estimation of mechanical and electrical systems.

C. OPTIMIZATION STRATEGIES

Computational intelligence-based optimization strategies are widely used to obtain optimal solutions to several problems of humankind. Metaheuristics are one of the prominent computational intelligence-based optimization strategies that are problem independent in nature. Meta-heuristics are generally classified into three main classes viz. evolutionary, physics-based, and swarm intelligence algorithms. Genetic Algorithm (GA) and Particle Swarm Optimization (PSO) are some of the most popular algorithms [53]. These algorithms have achieved more efficient results for various problems such as availability optimization of process industries. Also, GA and PSO are not influenced by the size and non-linearity of problems [49]. There are many other algorithms such as Chimp optimization, dynamic Levy flight chimp, and weighted Chimp optimization [54]–[60], [62]–[66] that can be applied in the future for estimating their performances in availability computations of STPP.

1) SIMULATION ENVIRONMENT

For simulating the experiments, we have used MATLAB R2019a on the Windows 10 64-bit operating system with 8 GB of RAM and Intel Core i5 8th generation CPU.

2) GENETIC ALGORITHM

GA is one of the well-known Evolutionary Computation (EC) approaches that is inspired by the biological evolution process [50], [51]. The process of EC is mainly characterized by the fitness computation of individuals who participate in achieving global optimization. Individuals with fitness greater than the specified threshold are retained for further evolution. Once the problem is encoded using decision parameters, the optimum solution can be obtained. GA starts by generating an initial random population based on initialization of values of decision parameters followed by computation of fitness of individuals as depicted in Figure 3.

The overall search process comprises of the following steps:

1. Problem encoding and generation of an initial random population (chromosomes) based on threshold values (lower bound and upper bound) of decision parameters.

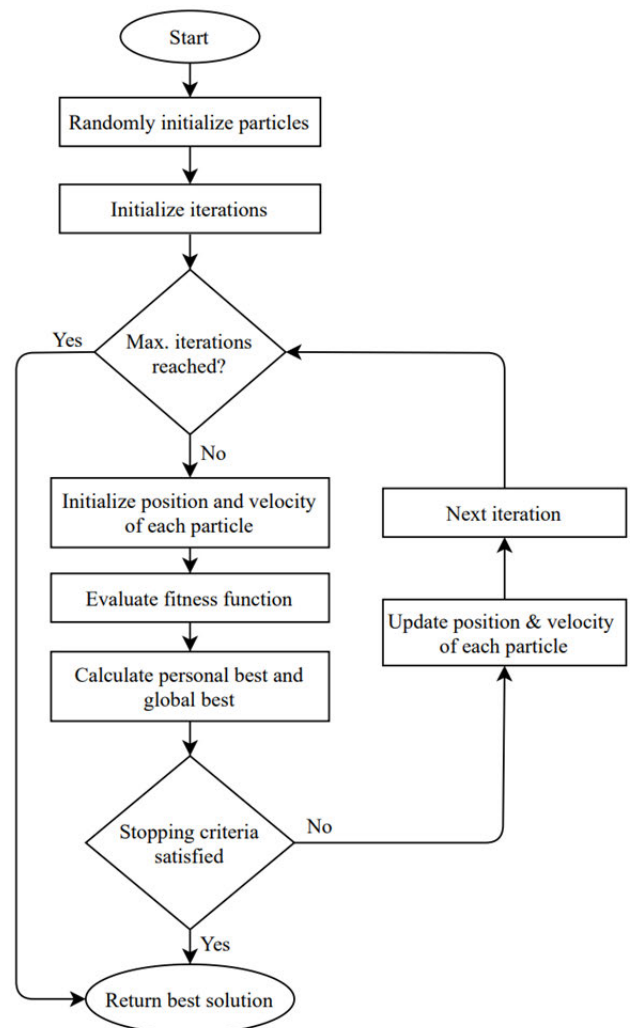


FIGURE 4. Flowchart of particle swarm optimization algorithm.

In our case, failure rates and repair rates of various subsystems of the cooling tower of steam turbine power plant are considered as decision parameters and their threshold values according to distributions (exponential in case of failure rates, whereas arbitrary for repair rates).

2. Fitness of individuals is evaluated using fitness function. In our case, the availability function (A_v) is considered as a fitness function that needs to be optimized.
3. Identification of terminating conditions (i.e., stopping criteria for convergence of algorithm after meeting specified constraints). If terminating conditions are satisfied, the algorithm converges, otherwise, it moves further.
4. Selection of parents (based on threshold values) and generation of new offspring by applying genetic operator (crossover and mutation).
5. Go to step 2.

Numerous variations of genetic operators (i.e., crossover and mutation) are presented in the literature. The main aim of these operators is to exchange genes so that a new population with high fitness values can be obtained. In a crossover, the parts of chromosomes are shuffled in different ways whereas in mutation new genetic material is introduced as a replacement of older one. One-point crossover and uniform mutation are adopted in this work for a generation of new offsprings.

3) PARTICLE SWARM OPTIMIZATION (PSO)

PSO developed by Eberhart and Kennedy [52] is one of the efficient swarm intelligence-based metaheuristic techniques that are inspired by birds' social behavior. The principal mechanism is the coordination of individuals for finding out optimal solutions to a problem. The term 'particles' refers to the individuals in a problem space, whereas swarm refers to their population. To obtain an optimal solution, particles move themselves to an appropriate position at a specified speed referred to as 'velocity'. For achieving a 'global best' solution, at every instance, each particle identifies its best position known as 'personal best'. This process is generally referred to as learning from experience. The algorithm converges upon either satisfying the stopping criteria or reaching maximum iterations as specified.

The position of the particles and their velocity is updated on every iteration. The working mechanism of PSO is depicted with the help of a flowchart in Figure 4. The basic mathematical foundations of PSO are given in Eq. 34 and 35. The position of a particle i at time t in the search space is denoted by $x_i(t)$. The new position of particle i is achieved by adding the velocity $v_i(t)$ to its current position, as stated in (34).

$$x_i(t+1) = x_i(t) + v_i(t+1) \quad (34)$$

Here, $v_i(t+1)$ indicates the combined value of inertia coefficient, cognitive component, and the social component as given in eq. 35

$$v_i(t+1) = w \cdot v_i(t) + c_1(p_i(t) - x_i(t)) + c_2(g(t) - x_i(t)) \quad (35)$$

In eq. (35), w indicates the inertia coefficient, $v_i(t)$ the initial velocity, $p_i(t)$ to be personal best, $g(t)$ indicates the global best, and c_1 and c_2 are acceleration coefficients. On every iteration, the position of individuals is getting updated based on various parameters viz. personal best, global best, and the velocity of movement from one position to another (towards global optimization).

4) ENCODING OF COOLING TOWER SUBSYSTEM USING GA AND PSO

To obtain the maximum availability of the cooling tower subsystem, the optimum values of failure and repair rates have been computed using GA and PSO. The availability function (Eq. 24) consisting of failure and repair rates of several cooling towers' subsystems (as given in Table 1) is considered as a fitness function. Optimizing the availability of cooling towers is measured as single-objective optimization subject to certain constraints of failure and repair rates. The optimization of the availability function has been checked against varying certain parameters of GA viz. population size, evolutions, crossover probability, and mutation probabilities, as shown in Tables 6-9.

The optimization of the availability function has been checked against varying certain parameters of PSO (i.e., iteration, population size, and damping ratio) by keeping the values of inertia weight, p-best, and g-best to be 1, 1.5, and 2, respectively, as shown in Tables 10-12.

D. MANN-WHITNEY U TEST

The Mann-Whitney U test is the non-parametric analogous to the independent t-test. It is used for testing the significant difference between two populations or to identify that both samples are drawn from the same distribution. If the null hypothesis is accepted, then both the samples have more or less the same values. The test statistic can be defined as:

$$U_1 = n_1 n_2 + \frac{n_1(n_1 + 1)}{2} - R_1$$

$$U_2 = n_1 n_2 + \frac{n_2(n_2 + 1)}{2} - R_2 \quad (36)$$

where n_1 and n_2 are sample sizes, R_1 and R_2 are rank sums of corresponding samples.

By using (36), the test statistics is as follows:

$$z = \frac{U_2 - \mu_{U_2}}{\sigma_{U_2}} \quad (37)$$

In the present analysis, a statistical comparison of GA and PSO results has been done using Eq. (37), as both the samples are independent and assumptions of parametric tests like normality, heteroscedasticity does not achieved [61].

VII. NUMERICAL RESULTS AND DISCUSSION

Here, the influence of variation in the failure rate of various subsystems of the cooling tower is estimated on availability (Eq. 24) and profit function (Eq. 32) for an arbitrary set

TABLE 2. Impact of variation in failure rates on availability with respect to hydraulic valves failure rate (ϑ_2).

ϑ_2	Initial value of parameter	$\vartheta_1 = 0.06$	$\vartheta_3 = 0.009$	$\vartheta_4 = 0.0055$	$\vartheta_5 = 0.035$	$\vartheta_6 = 0.15$	$\vartheta_7 = 0.052$
0.0045	0.786605	0.534392	0.659309	0.764870	0.583447	0.745722	0.415099
0.0055	0.779393	0.531053	0.654234	0.758049	0.579469	0.739237	0.413082
0.0065	0.772311	0.527756	0.649237	0.751348	0.575546	0.732863	0.411084
0.0075	0.765357	0.524500	0.644316	0.744765	0.571675	0.726598	0.409106
0.0085	0.758527	0.521283	0.639469	0.738296	0.567856	0.720440	0.407146
0.0095	0.751818	0.518105	0.634694	0.731938	0.564087	0.714385	0.405205
0.0105	0.745227	0.514967	0.629989	0.725689	0.560368	0.708431	0.403283
0.0115	0.738750	0.511865	0.625355	0.719546	0.556698	0.702575	0.401378
0.0125	0.732385	0.508802	0.620787	0.713506	0.553076	0.696816	0.399492
0.0135	0.726128	0.505774	0.616286	0.707567	0.549501	0.691150	0.397623

TABLE 3. Impact of variation in failure rates on profit with respect to hydraulic valves failure rate (ϑ_2).

ϑ_2	Initial value of parameter	$\vartheta_1 = 0.06$	$\vartheta_3 = 0.009$	$\vartheta_4 = 0.0055$	$\vartheta_5 = 0.035$	$\vartheta_6 = 0.15$	$\vartheta_7 = 0.052$
0.0045	2646.4220	1637.5682	2137.2354	2559.4798	1833.7877	2482.8881	1160.3965
0.0055	2617.5714	1624.2134	2116.9369	2532.1947	1817.8776	2456.9462	1152.3274
0.0065	2589.2451	1611.0244	2096.9485	2505.3919	1802.1829	2431.4516	1144.3362
0.0075	2561.4289	1597.9981	2077.2632	2479.0589	1786.6994	2406.3930	1136.4220
0.0085	2534.1092	1585.1316	2057.8740	2453.1832	1771.4228	2381.7591	1128.5837
0.0095	2507.2727	1572.4220	2038.7744	2427.7533	1756.3489	2357.5392	1120.8200
0.0105	2480.9068	1559.8664	2019.9579	2402.7575	1741.4737	2333.7231	1113.1300
0.0115	2454.9993	1547.4620	2001.4183	2378.1849	1726.7934	2310.3007	1105.5127
0.0125	2429.5381	1535.2061	1983.1495	2354.0249	1712.3042	2287.2624	1097.9669
0.0135	2404.5120	1523.0960	1965.1456	2330.2671	1698.0023	2264.5987	1090.4918

of parametric values. The initial parametric values are as follows:

$$\begin{aligned} \vartheta_1 &= 0.006, & \vartheta_3 &= 0.0009, & \vartheta_4 &= 0.00075, & \vartheta_5 &= 0.0018, \\ \vartheta_6 &= 0.0054, & \vartheta_7 &= 0.0008, & \sigma_1 &= 0.09, & \sigma_2 &= 0.085, \\ \sigma_3 &= 0.033, & \sigma_4 &= 0.026, & \sigma_5 &= 0.075, & \sigma_6 &= 0.066, \\ \sigma_7 &= 0.045 \end{aligned}$$

The variation is observed concerning hydraulic valves failure rate (ϑ_2). It is revealed that hydro turbine, cooling tower pump, and standpipe are the most sensitive components in the cooling tower. By changing the value of $\vartheta_1 = 0.006$ to $\vartheta_1 = 0.06$ and keeping rest values as constant, it is revealed from Table 2, that the availability of cooling tower reduces

up to 0.534392 while in a subsystem where the provision of standby unit is given, the availability does not show high variation. From Table 3, the same behavior is depicted for the profit function. The availability and profit function values decline by increasing the failure rates of all the components. Availability of the system decreases by 5.35% approximately with the increase in failure rate $\vartheta_1 = 0.006$ to $\vartheta_1 = 0.06$. Similarly, the availability of the system decreases 6.53%, 7.49%, 5.82 %, 7.32%, and 4.21% approximately with the increase in the failure rate of ϑ_3 from 0.0009 to 0.009, ϑ_4 from 0.00075 to 0.0055, ϑ_5 from 0.0018 to 0.035, ϑ_6 from 0.0054 to 0.15 and ϑ_7 from 0.0008 to 0.052 respectively and in Table 3, it is revealed that profit of the system decreases 6.99% approximately with the increase in failure rate ϑ_1 from 0.006 to 0.06. Similarly, the profit of the system

TABLE 4. Impact of variation in repair rates on availability with respect to hydraulic valves repair rate (ϑ_2).

σ_2	Initial value of parameter	$\sigma_1 = 2.1$	$\sigma_3 = 0.95$	$\sigma_4 = 0.2$	$\sigma_5 = 1.9$	$\sigma_6 = 0.95$	$\sigma_7 = 0.81$
0.085	0.786605	0.828174	0.803239	0.787098	0.801133	0.836714	0.797133
0.095	0.790069	0.832014	0.806850	0.790565	0.804725	0.840634	0.800690
0.105	0.792895	0.835149	0.809798	0.793395	0.807657	0.843834	0.803593
0.115	0.795245	0.837756	0.812249	0.795748	0.810096	0.846496	0.806007
0.125	0.797229	0.839959	0.814320	0.797735	0.812155	0.848745	0.808046
0.135	0.798928	0.841844	0.816092	0.799435	0.813918	0.850670	0.809790
0.145	0.800398	0.843477	0.817626	0.800907	0.815444	0.852337	0.811301
0.155	0.801683	0.844904	0.818967	0.802194	0.816777	0.853794	0.812621
0.165	0.802815	0.846162	0.820148	0.803328	0.817953	0.855079	0.813784
0.175	0.803821	0.847279	0.821198	0.804335	0.818997	0.856220	0.814818

TABLE 5. Impact of variation in repair rates on profit with respect to hydraulic valves repair rate (ϑ_2).

σ_2	Initial value of parameter	$\sigma_1 = 2.1$	$\sigma_3 = 0.95$	$\sigma_4 = 0.2$	$\sigma_5 = 1.9$	$\sigma_6 = 0.95$	$\sigma_7 = 0.81$
0.085	2646.4220	2812.6959	2712.9548	2648.3902	2704.5308	2846.8565	2688.5336
0.095	2660.2752	2828.0555	2727.4014	2662.2609	2718.9016	2862.5353	2702.7610
0.105	2671.5794	2840.5943	2739.1919	2673.5793	2730.6299	2875.3357	2714.3717
0.115	2680.9789	2851.0238	2748.9970	2682.9906	2740.3831	2885.9837	2724.0269
0.125	2688.9176	2859.8352	2757.2792	2690.9394	2748.6215	2894.9801	2732.1822
0.135	2695.7115	2867.3777	2764.3679	2697.7419	2755.6725	2902.6814	2739.1619
0.145	2701.5916	2873.9071	2770.5036	2703.6295	2761.7755	2909.3486	2745.2031
0.155	2706.7306	2879.6147	2775.8664	2708.7750	2767.1097	2915.1769	2750.4832
0.165	2711.2603	2884.6465	2780.5937	2713.3106	2771.8118	2920.3151	2755.1375
0.175	2715.2831	2889.1157	2784.7922	2717.3385	2775.9878	2924.8791	2759.2711

TABLE 6. Steady-state availability with respect to population size having no. of evolutions 400, mutation probability 0.65, and crossover probability 0.85.

Pop. Size	Availability	ϑ_1	ϑ_2	ϑ_3	ϑ_4	ϑ_5	ϑ_6	ϑ_7	σ_1	σ_2	σ_3	σ_4	σ_5	σ_6	σ_7
15	0.9884	0.0054	0.0020	0.0018	0.0001	0.0019	0.0014	0.0002	0.6008	0.2800	0.0128	0.0406	0.2385	0.3472	0.0134
30	0.9669	0.0217	0.0058	0.0014	0.0002	0.0003	0.0008	0.0001	1.2517	1.7640	0.0110	0.0773	0.4982	0.0852	0.0430
45	0.9613	0.0059	0.0162	0.0004	0.0002	0.0008	0.0083	0.0011	0.9537	0.5507	0.3407	0.0062	0.6298	0.4730	0.0211
60	0.9803	0.0043	0.0011	0.0008	0.0013	0.0011	0.0015	0.0001	0.1392	0.5411	0.0732	0.1172	0.1651	0.303	0.0195
75	0.9811	0.0017	0.0026	0.0001	0.0002	0.0004	0.0021	0.0013	0.3716	0.3448	0.1408	0.0178	0.5711	0.3096	0.0022
90	0.9170	0.0106	0.0001	0.0009	0.0025	0.0039	0.0014	0.0006	0.3652	0.1608	0.0526	0.0459	1.4511	0.4553	0.0140
105	0.9791	0.0057	0.0020	0.0003	0.0001	0.0002	0.0004	0.0002	0.5073	0.3460	0.0541	0.0618	0.2217	0.3733	0.0628
120	0.9825	0.0003	0.0027	0.0005	0.0003	0.0019	0.0002	0.0007	0.2273	0.3809	0.1069	0.0642	0.6044	0.3378	0.0208
135	0.9705	0.0004	0.0037	0.0003	0.0011	0.0020	0.0007	0.0001	0.1389	0.6843	0.0909	0.0706	0.2471	0.4544	0.0830

decreases 8.05%, 8.95%, 7.40%, 8.79%, and 6.02% approximately with the increase in the failure rate of ϑ_3 from 0.0009 to 0.009, ϑ_4 from 0.00075 to 0.0055, ϑ_5 from 0.0018 to 0.035, ϑ_6 from 0.0054 to 0.15 and ϑ_7 from 0.0008 to 0.052 respectively.

From Table 4, it is found that the availability of the system shows a 2.31% enhancement along with the increase in repair rate σ_1 from 0.09 to 2.1. Also, the availability of the system is improved by 2.23%, 2.19%, 2.23%, 2.33%, and 2.22%, respectively with the increase in repair rate σ_3 from 0.033

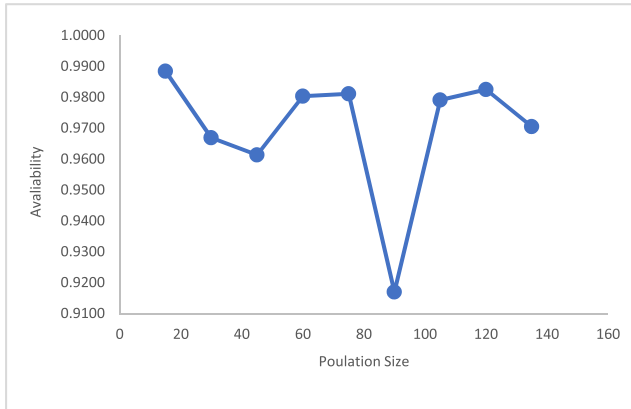


FIGURE 5. Availability vs. population size in GA.

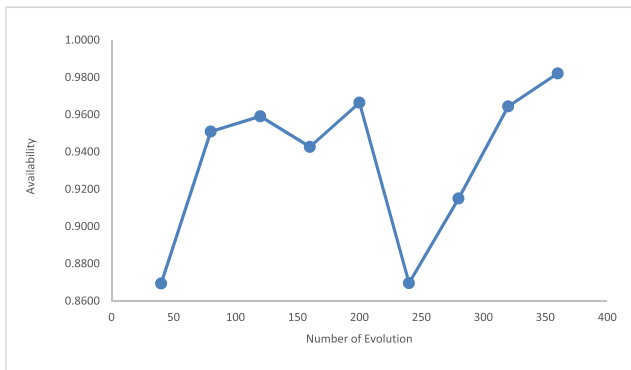


FIGURE 6. Availability vs. number of evolutions in GA.

to 0.95, σ_4 from 0.26 to 0.2, σ_5 from 0.075 to 1.9, σ_6 from 0.066 to 0.95 and σ_7 from 0.045 to 0.81 respectively and Table 5 reflected that profit of the system increases 2.72% approximately with the increase in repair rate σ_1 from 0.09 to 2.1. Similarly, profit of the system increases 2.65%, 2.60%, 2.64%, 2.74%, and 2.63% approximately with the increase in repair rate σ_3 from 0.033 to 0.95, σ_4 from 0.26 to 0.2, σ_5 from 0.075 to 1.9, σ_6 from 0.066 to 0.95 and σ_7 from 0.045 to 0.81 respectively.

TABLE 7. Steady-state availability with respect to the number of evolutions having population size 60, mutation probability 0.65, and crossover probability 0.85.

Evolution	Availability	ϑ_1	ϑ_2	ϑ_3	ϑ_4	ϑ_5	ϑ_6	ϑ_7	σ_1	σ_2	σ_3	σ_4	σ_5	σ_6	σ_7
40	0.8694	0.0012	0.0035	0.0016	0.0007	0.0041	0.0026	0.0001	0.5906	0.1418	0.0454	0.0038	0.8776	0.5504	0.0222
80	0.9509	0.0102	0.0165	0.0002	0.0005	0.0004	0.0011	0.0013	0.4836	0.5711	0.0434	0.0278	0.8630	0.2640	0.0474
120	0.9591	0.0026	0.0029	0.0008	0.0003	0.0014	0.0035	0.0007	0.1773	0.7482	0.0164	0.0021	0.5800	0.3700	0.0175
160	0.9427	0.0028	0.0017	0.0010	0.0003	0.0068	0.0019	0.0004	0.4042	0.2472	0.0658	0.0672	0.5669	0.8678	0.0105
200	0.9664	0.0038	0.0043	0.0002	0.0005	0.0066	0.0002	0.0007	0.3188	0.8639	0.0762	0.0667	0.3105	0.1795	0.0915
240	0.8696	0.0012	0.0072	0.0001	0.001	0.0006	0.0014	0.0004	0.7811	0.4142	0.0484	0.0565	0.0848	0.3758	0.0287
280	0.9150	0.0091	0.0033	0.0006	0.0006	0.0042	0.0015	0.0006	0.4307	0.2108	0.0556	0.0800	0.2804	0.7236	0.0143
320	0.9644	0.0016	0.0040	0.0006	0.0003	0.0004	0.0001	0.0003	0.0591	0.1568	0.0416	0.0595	0.2350	0.5718	0.0192
360	0.9821	0.0023	0.0042	0.0010	0.0001	0.0104	0.0033	0.0017	0.6898	0.5075	0.0251	0.0050	1.3364	0.6845	0.0501

From Tables (4-5), it is observed that water spray pumps and motor valves are highly influential components. Any increment in their repair rate significantly contributes to increasing system availability and profit. Availability showed a highly inclined trend when the variation was made in repair rates as given in Table 4.

As depicted in Table 6, the availability of the cooling tower subsystem has been computed by varying the population size. The values of evolution, mutation, and crossover are kept fixed at 400, 0.65, and 0.85, respectively. It is observed that the maximum availability has been obtained when the population size is 15. An increase in population results in decreasing overall availability.

The optimum values of failure and repair rates of different subsystems can also be seen from Table 6 against maximum availability when the size of the population is 15. The relationship of availability vs. population in GA as computed for the cooling tower subsystem is also depicted in Figure 5.

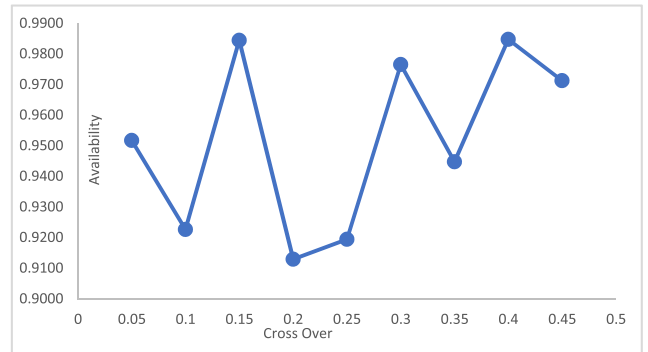


FIGURE 7. Availability vs. crossover probability in GA.

In GA, the impact of evolution has also been observed towards optimizing the availability computations of cooling tower subsystems. As shown in Table 7, the availability of the cooling tower subsystem has been computed by varying evolutions. The values of population, mutation, and crossover are kept fixed at 60, 0.65, and 0.85, respectively. It is observed that the maximum availability has been obtained on 360 evaluations. An increase in evolution results in an increase in

TABLE 8. Steady-state availability with respect to crossover probability having population size 60, number of evolutions 400, and mutation probability 0.65.

Cross Over	Availability	ϑ_1	ϑ_2	ϑ_3	ϑ_4	ϑ_5	ϑ_6	ϑ_7	σ_1	σ_2	σ_3	σ_4	σ_5	σ_6	σ_7
0.05	0.9517	0.0008	0.0085	0.0038	0.0011	0.0034	0.0003	0.0006	0.0780	0.7544	0.0393	0.0751	0.2620	0.3610	0.0457
0.1	0.9226	0.0068	0.0004	0.0003	0.0004	0.0020	0.0001	0.0005	0.7117	0.3349	0.0884	0.0460	1.2213	0.5637	0.0100
0.15	0.9844	0.0016	0.0002	0.0002	0.0005	0.0014	0.0078	0.0003	0.3429	0.0297	0.1121	0.0043	0.7934	0.7366	0.0222
0.2	0.9129	0.0119	0.0032	0.0009	0.0007	0.0003	0.0001	0.0002	0.4359	0.4919	0.0307	0.0241	0.4388	0.4623	0.0208
0.25	0.9194	0.0007	0.0008	0.0001	0.0001	0.0004	0.0014	0.0004	0.9118	0.2238	0.0363	0.0729	0.5782	0.2911	0.0817
0.3	0.9765	0.0019	0.0008	0.0008	0.0002	0.0001	0.0005	0.0002	1.0011	0.6762	0.0081	0.0017	0.5574	0.7546	0.0193
0.35	0.9447	0.0095	0.0014	0.0008	0.0001	0.0052	0.0026	0.0009	1.0211	0.0757	0.0614	0.0353	0.6444	0.3696	0.0220
0.4	0.9847	0.0044	0.0043	0.0001	0.0001	0.0013	0.002	0.0001	0.3715	0.392	0.0045	0.0742	0.1965	0.8359	0.0203
0.45	0.9712	0.0028	0.0038	0.0001	0.0001	0.0002	0.0004	0.0005	0.3840	1.2576	0.0182	0.0056	0.0269	0.3422	0.0320

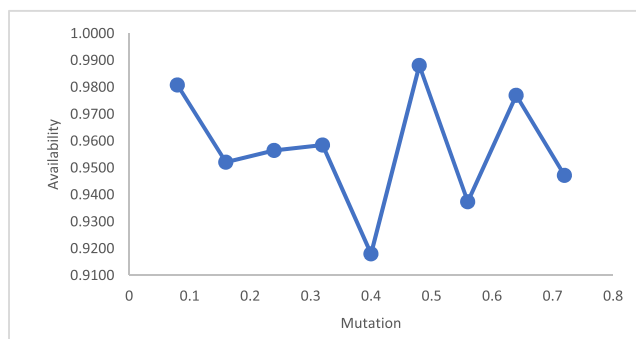


FIGURE 8. Availability vs. mutation probability in GA.

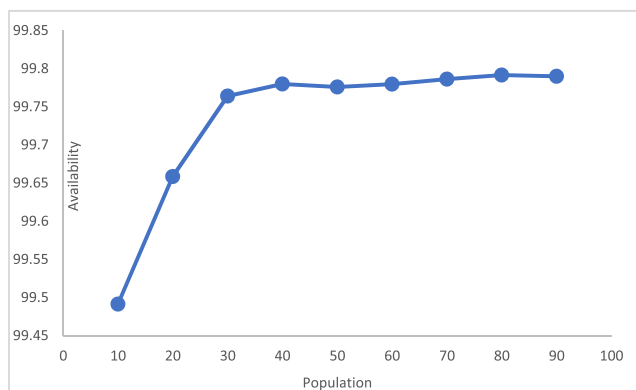


FIGURE 9. Availability vs. number of iterations in PSO.

overall availability. The optimum values of failure and repair rates of different subsystems can also be seen from Table 7 against maximum availability when the value of evolution is 360. The relationship of availability vs. evolutions in GA as computed for cooling tower subsystem is also depicted in Figure6.

The impact of crossover rate has also been observed towards optimizing availability computations of cooling tower subsystems. As shown in Table 8, the availability of the cooling tower subsystem has been computed by varying the crossover rate. The population, evolution, and mutation values are kept fixed at 60, 400, and 0.65. It is observed that the maximum availability has been obtained when the value

of crossover is 0.4. The optimum values of failure and repair rates of different subsystems can also be seen from Table 8 against maximum availability when the value of crossover is 0.4. The relationship of availability vs. crossover probability in GA as computed for the cooling tower subsystem is also depicted in Figure 7.

The impact of mutation rate has also been observed towards optimizing availability computations of cooling tower subsystems. As shown in Table 9, the availability of the cooling tower subsystem has been computed by varying the crossover rate. The values of population, evolution, and crossover are kept fixed at 60, 400, and 0.65, respectively. It is observed that the maximum availability has been obtained when the value of mutation is 0.48. The optimum values of failure and repair rates of different subsystems can also be seen from Table 9 against maximum availability when the value of mutation is 0.48. The relationship of availability vs. mutation probability in GA as computed for the cooling tower subsystem is also depicted in Figure 8.

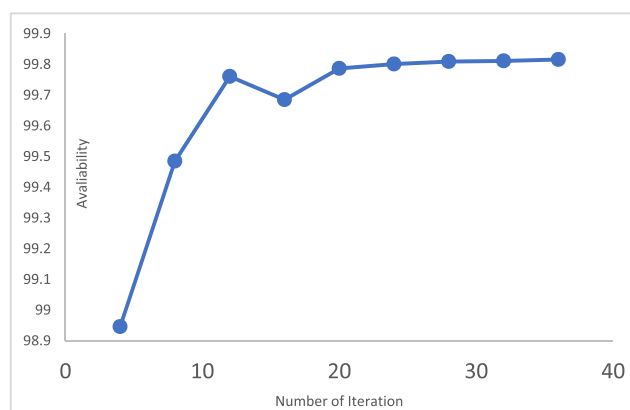


FIGURE 10. Availability vs. population size in PSO.

In PSO, the impact of iterations over-optimizing availability computations of cooling tower subsystems has been observed, as shown in Table 10. The values of other parameters such as population size, inertia weight, damping ratio, p-best, and g-best are kept at 60, 1, 0.9, 1.5, and 2,

TABLE 9. Steady-state availability with respect to mutation probability having population size 60, number of evolutions 400, and crossover probability 0.85.

Mutation	Availability	ϑ_1	ϑ_2	ϑ_3	ϑ_4	ϑ_5	ϑ_6	ϑ_7	σ_1	σ_2	σ_3	σ_4	σ_5	σ_6	σ_7
0.08	0.9808	0.0028	0.0011	0.0016	0.0001	0.0001	0.0017	0.0006	0.4565	0.1093	0.1692	0.0032	0.1695	0.4058	0.0256
0.16	0.9521	0.0126	0.0015	0.0005	0.0003	0.0008	0.0019	0.0005	0.6976	1.1517	0.0589	0.0961	0.2767	0.4842	0.0065
0.24	0.9565	0.0001	0.0008	0.0001	0.0002	0.0014	0.0031	0.0032	0.3276	0.5014	0.0420	0.1431	0.4405	0.6955	0.0075
0.32	0.9585	0.0036	0.0092	0.0009	0.0002	0.0035	0.0027	0.0002	0.6202	0.3839	0.0329	0.0281	0.1957	0.5474	0.0090
0.4	0.9180	0.0124	0.0058	0.0002	0.0007	0.0008	0.0014	0.0003	0.3343	0.2292	0.1642	0.0033	0.1628	0.3489	0.0349
0.48	0.9881	0.0011	0.0003	0.0002	0.0005	0.0020	0.0006	0.0009	0.9069	0.3459	0.1666	0.0229	0.2023	0.4327	0.0859
0.56	0.9374	0.0026	0.0002	0.0002	0.0002	0.0072	0.0004	0.0021	0.4916	0.1040	0.0899	0.0171	0.3580	0.2357	0.0434
0.64	0.9770	0.0004	0.0003	0.0005	0.0001	0.0033	0.0002	0.0005	2.1925	0.0648	0.0005	0.1173	1.1217	0.2585	0.0208
0.72	0.9472	0.0058	0.0095	0.0012	0.0002	0.0010	0.0011	0.0004	0.5024	0.2378	0.0085	0.1105	0.1952	0.2823	0.0063

TABLE 10. Steady-state availability with respect to the number of iterations having population size 60, inertia weight 1, damping ratio 0.9, p-best 1.5, and g-best 2.

Iteration	Availability	ϑ_1	ϑ_2	ϑ_3	ϑ_4	ϑ_5	ϑ_6	ϑ_7	σ_1	σ_2	σ_3	σ_4	σ_5	σ_6	σ_7
4	.989461	0.0639	0.0121	0.0038	0.0019	0.0726	0.0056	7.57E-04	0.4906	0.5042	0.0455	0.1889	0.7916	0.4042	0.2791
8	.99485	0.0029	0.0146	0.0069	0.0031	0.0614	0.0166	0.0045	0.7363	1.1315	0.7871	0.3864	0.5169	0.8791	0.583
12	.99761	0.0506	0.001	0.003	0.0012	0.0041	0.0123	0.0038	0.9628	0.9145	0.5183	0.0287	0.6638	0.8058	0.3405
16	.996853	0.0389	0.0155	0.0064	0.0067	0.0838	0.0066	0.0016	0.1534	0.3214	0.0164	0.7853	0.9522	0.6002	0.434
20	.997872	0.0597	0.0411	0.0081	0.004	0.0532	0.0023	0.0056	0.5367	0.7316	0.0914	0.5991	0.6027	0.7494	0.3535
24	.998012	0.0718	0.0131	0.0043	0.0041	0.0596	0.0017	0.0056	0.9265	0.2654	0.7243	0.296	0.708	0.3747	0.1444
28	.998092	0.0092	0.063	0.0056	0.0024	0.0237	0.0206	0.0013	1.0073	0.5438	0.3903	0.5557	0.8282	0.8168	0.0764
32	.998115	0.0544	0.0256	0.0037	0.0025	0.0536	0.0019	7.18E-04	1.1854	1.0198	0.182	0.2833	0.6328	0.4815	0.2337
36	.998162	0.0203	0.0052	0.0076	7.07E-04	0.0469	0.0035	0.003	0.6199	0.7525	0.2067	0.0733	0.2303	0.8826	0.3024

TABLE 11. Steady-state availability with respect to population size having a number of iterations 20, inertia weight 1, damping ratio 0.9, p-best 1.5, and g-best 2.

Population	Availability	ϑ_1	ϑ_2	ϑ_3	ϑ_4	ϑ_5	ϑ_6	ϑ_7	σ_1	σ_2	σ_3	σ_4	σ_5	σ_6	σ_7
10	.994914	0.0777	0.0268	0.0065	0.0042	0.0289	0.0406	0.00083	0.4813	1.1463	0.8453	0.3704	0.8094	0.6824	0.9915
20	.996584	0.0507	0.0244	0.0039	0.0051	0.0148	0.0603	0.0023	0.8625	0.9834	0.6489	0.2884	0.1555	0.8084	0.2893
30	.99764	0.0146	0.0398	0.0061	0.0041	0.0233	0.006	0.0068	0.4023	0.6969	0.7334	0.2341	0.1223	0.6669	0.0288
40	.997798	0.0373	0.0103	0.0093	0.0032	0.0026	0.0201	0.0041	1.0038	0.1913	0.4528	0.2419	0.0562	0.6459	0.7118
50	.997759	0.0642	0.0451	0.0045	0.0033	0.0158	0.003	0.0054	0.5651	0.7956	0.4247	0.2204	0.446	0.4404	0.5697
60	.997795	0.005	0.053	0.0053	0.0033	0.0025	0.0081	0.004	0.8244	0.2063	0.7794	0.6131	0.0854	0.7374	0.4284
70	.997862	0.0354	0.0458	0.0058	0.0051	0.0376	0.0131	0.0066	0.1271	0.3936	0.3279	0.4	0.4465	0.6972	0.9988
80	.997916	0.0406	0.0028	0.0063	0.0059	0.0123	0.0193	0.000884	1.1383	0.9247	0.5968	0.1449	0.9512	0.8745	0.0076
90	.997899	0.0286	0.0092	0.0033	0.0029	0.0247	0.0188	0.0058	0.4028	1.1211	0.4114	0.0449	0.7937	0.4754	0.133

respectively. It is observed that the maximum availability has been obtained when the value of iteration is 28.

The optimum values of failure and repair rates of different subsystems can also be seen from table 10 against maximum availability when the value of iteration is 28. The relationship of availability vs. iteration in PSO as computed for the cooling tower subsystem is also depicted in Figure 9.

In PSO, the impact of population size over optimizing the availability computations of cooling tower subsystems has also been observed, as shown in Table 11. The values of

other parameters such as iteration, inertia weight, damping ratio, p-best, and g-best are kept at 20, 1, 0.9, 1.5, and 2, respectively. It is observed that the maximum availability has been obtained when the value of the population is 80. The optimum values of failure and repair rates of different subsystems can also be seen from Table 11 against maximum availability when the value of the population is 80. The relationship of availability vs. iteration in PSO as computed for the cooling tower subsystem is also depicted in Figure 10.

TABLE 12. Steady-state availability with respect to population size having a number of iterations 20, inertia weight 1, population size 60, p-best 1.5, and g-best 2.

Damping Ratio	Availability	ϑ_1	ϑ_2	ϑ_3	ϑ_4	ϑ_5	ϑ_6	ϑ_7	σ_1	σ_2	σ_3	σ_4	σ_5	σ_6	σ_7
0.06	.997974	0.0162	0.0492	0.0056	0.0069	0.0213	0.0189	0.0067	1.0366	0.6083	0.7335	0.2233	0.6831	0.7847	0.5962
0.12	.998049	0.0438	0.0081	0.0087	0.0054	0.06	0.0092	0.0025	0.2785	0.9208	0.1429	0.3917	0.7961	0.7797	0.0361
0.18	.997959	0.0135	0.0367	0.0042	0.0076	0.029	0.0182	0.0024	0.272	0.3633	0.2389	0.3436	0.8931	0.7637	0.6045
0.24	.997829	0.0433	0.0057	0.0047	0.0035	0.0666	0.0086	0.0042	1.0949	0.9824	0.2213	0.1435	0.2984	0.1924	0.8504
0.3	.997952	0.0536	0.029	0.0058	0.003	0.0245	0.0035	0.006	0.5734	0.4386	0.1936	0.0773	0.3576	0.5286	0.7803
0.36	.99806	0.0281	0.0364	0.009	0.0045	0.022	0.042	0.0025	0.601	0.489	0.7217	0.2335	0.5672	0.7736	0.1141
0.42	.997701	0.0625	0.023	0.0068	0.0073	0.0626	0.0121	0.0034	0.6913	0.8891	0.7733	0.0532	0.2591	0.5377	0.7408
0.48	.997905	0.0048	0.0021	0.0072	0.0016	0.0575	0.0292	0.0068	0.753	0.4459	0.7826	0.3545	0.5459	0.8919	0.4363
0.54	.997994	0.0365	0.0429	0.002	0.0039	0.0193	0.0053	0.0048	0.4614	1.0899	0.3743	0.0342	0.6672	0.8768	0.3757

TABLE 13. Sensitivity analysis of steady-state availability with respect to failure rates.

$\frac{\partial A}{\partial \theta_1}$	$\frac{\partial A}{\partial \theta_2}$	$\frac{\partial A}{\partial \theta_3}$	$\frac{\partial A}{\partial \theta_4}$	$\frac{\partial A}{\partial \theta_5}$	$\frac{\partial A}{\partial \theta_6}$	$\frac{\partial A}{\partial \theta_7}$
-0.39196	-0.41502	-1.06899	-6.35341	-0.47036	-0.5345	-0.78393
-0.39024	-0.41319	-1.06428	-6.33854	-0.46828	-0.53214	-0.78047
-0.38852	-0.41138	-1.0596	-6.32375	-0.46623	-0.5298	-0.77704
-0.38682	-0.40957	-1.05496	-6.30902	-0.46418	-0.52748	-0.77364
-0.38513	-0.40778	-1.05034	-6.29435	-0.46215	-0.52517	-0.77025
-0.38344	-0.406	-1.04576	-6.27976	-0.46013	-0.52288	-0.76689
-0.38177	-0.40423	-1.0412	-6.26523	-0.45813	-0.5206	-0.76355
-0.38011	-0.40247	-1.03667	-6.25077	-0.45614	-0.51834	-0.76023
-0.37846	-0.40073	-1.03218	-6.23638	-0.45416	-0.51609	-0.75693
-0.37683	-0.39899	-1.02771	-6.22205	-0.45219	-0.51385	-0.75365

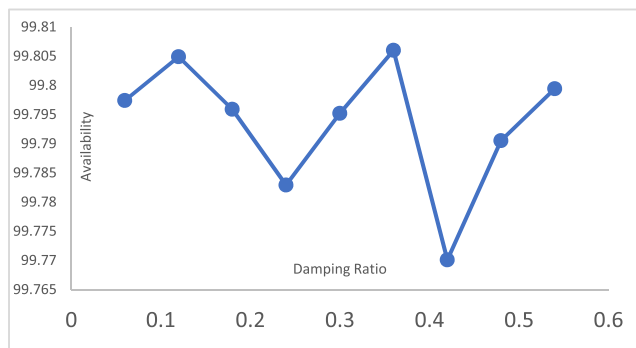


FIGURE 11. Availability vs. damping ratio in PSO.

In PSO, the impact of damping ratio over optimizing the availability computations of cooling tower subsystems have also been observed, as shown in Table 12. The values of other parameters such as iterations, inertia weight, population, p-best, and g-best are kept at 20, 1, 60, 1.5, and 2, respectively. It is observed that the maximum availability has been obtained when the value of the damping ratio is 0.36. The optimum values of failure and repair rates of different subsystems can also be seen from Table 12 against maximum availability when the value of damping ratio is 0.36. The relationship of availability vs. iteration in PSO as computed for the cooling tower subsystem is also depicted in Figure 11.

The availability computations of cooling tower subsystems are computed using two well-known population-based metaheuristic approaches, viz. GA and PSO. To obtain the

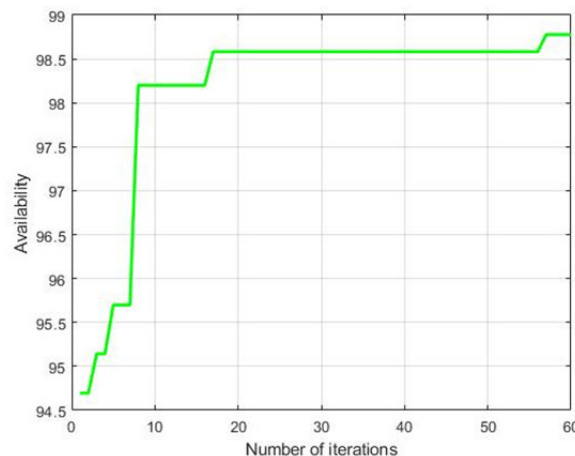


FIGURE 12. Availability vs. number of iterations in GA.

optimum availability, various parameters of these approaches have been evaluated by varying their values.

It is observed that PSO outperforms GA in terms of availability computations in very few iterations, as shown in Figures 12 and 13. Figure 12 and 13 depicts the availability of the cooling tower subsystem concerning the number of iterations performed by GA and PSO respectively. As shown in figure 13, the maximum availability of 99.8% is achieved by PSO in just 18 iterations, whereas GA took 60 iterations in achieving a maximum availability of only 98.8%. PSO is efficient in providing optimum values of failure and repair rates of cooling tower subsystems in achieving maximum

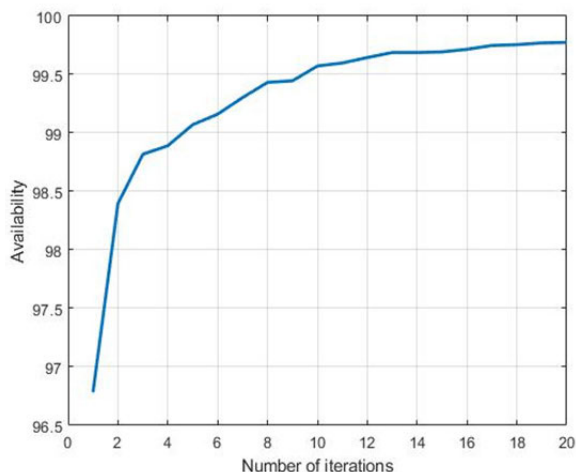


FIGURE 13. Availability vs. number of iterations in PSO.

availability of the whole system in a few iterations. Table 13 shows that the failure rate of automatic deaerator valves is most sensitive, and the operation of this component needs high attention. The comparison of GA and PSO availability results is statistically validated using Mann-Whitney U-test. The cooling tower availability corresponding to population size has been statistically analyzed at a 5% level of significance, under null hypothesis: both algorithms are equally effective and alternative hypothesis: PSO performs better than GA. Using SPSS (Version 21) software the absolute calculated value of test statistics $z = 3.576$ while absolute critical z value is 1.645 at a 5% level of significance. Here, the calculated value is greater than the tabulated value so cannot accept the null hypothesis. So, it is statistically significant that PSO outperforms GA.

VIII. CONCLUSION

The failure mechanism and repair policies have a significant impact on the system's operational availability and profit function. A mathematical model for the cooling tower in a steam turbine power plant (STPP) has been developed using the Markov birth-death process and supplementary variable technique. A critical evaluation of the model was carried out, and the impact of various failure and repair rates has been investigated. It was revealed that the standpipe, hydro turbine, and cooling water pump failure rates are very sensitive. While repair rates of motor valves and water supply systems show steep increments concerning their repair rate. The availability and profit decline concerning the failure rate of all subsystems. The sensitivity analysis shows that the failure rate of Automatic Deaerator Valves (ADV) is highly influential that can reduce the overall operational availability of the system. The overall availability was optimized using two well-known metaheuristic approaches viz. Genetic Algorithm (GA) and Particle Swarm Optimization (PSO). GA and PSO proved to be more efficient for such types of problems. It was revealed from the experimental evaluations that the PSO outperforms GA in optimizing the availability computations. Optimum

availability of cooling tower achieved through GA was found to be 0.9884, whereas through PSO the same was recorded to be 0.9980. It has been observed that the convergence rate of PSO was very fast in achieving the optimum availability of cooling towers as compared to GA. Therefore, the present model and derived results are very helpful to STPP designers to develop highly reliable and available systems. Further, GA, PSO, and other metaheuristic techniques can be utilized to obtain the optimum availability of various process industries, i.e., Paper and Pulp, Shoe Manufacturing, Sugar Industry, and Sewage Treatment Plant.

CONFLICTS OF INTEREST

The authors would like to confirm there are no conflicts of interest regarding the study.

REFERENCES

- [1] H. H. Reichert, "Simulation of power plants steam generators and cooling towers with artificial neural network," School Eng., Graduate Program Mech. Eng., Federal Univ. Rio Grande do Sul, Porto Alegre, Brazil, Tech. Rep., 2019. [Online]. Available: <https://lume.ufrgs.br/handle/10183/212374>
- [2] Y. Zhi, W. Weiqing, W. Haiyun, and H. Khodaei, "Improved butterfly optimization algorithm for CCHP driven by PEMFC," *Appl. Thermal Eng.*, vol. 173, Jun. 2020, Art. no. 114766.
- [3] R. Baños, F. Manzano-Agugliaro, F. Montoya, C. Gil, A. Alcayde, and J. Gómez, "Optimization methods applied to renewable and sustainable energy: A review," *Renew. Sustain. Energy Rev.*, vol. 15, no. 4, pp. 1753–1766, 2011.
- [4] J. Mahmoudimehr and P. Sebghati, "A novel multi-objective dynamic programming optimization method: Performance management of a solar thermal power plant as a case study," *Energy*, vol. 168, pp. 796–814, Feb. 2018.
- [5] M. H. K. Manesh and M. Ameryan, "Optimal design of a solar-hybrid cogeneration cycle using cuckoo search algorithm," *Appl. Thermal Eng.*, vol. 102, pp. 1300–1313, Jun. 2016.
- [6] Y. Wang, L. Yu, B. Nazir, L. Zhang, and H. Rahmani, "Innovative geothermal-based power and cooling cogeneration system; Thermodynamic analysis and optimization," *Sustain. Energy Technol. Assessments*, vol. 44, Apr. 2021, Art. no. 101070.
- [7] M. Liu, L. Chen, K. Jiang, X. Zhou, Z. Zhang, H. Zhou, W. Wang, L. Yang, and Y. Niu, "Investigation of thermo-flow characteristics of natural draft dry cooling systems designed with only one tower in 2×660 MW power plants," *Energies*, vol. 14, no. 5, p. 1308, Feb. 2021.
- [8] H. Alimoradi, M. Soltani, P. Shahali, F. M. Kashkooli, R. Larizadeh, K. Raahemifar, M. Adibi, and B. Ghasemi, "Experimental investigation on improvement of wet cooling tower efficiency with diverse packing compaction using ANN-PSO algorithm," *Energies*, vol. 14, no. 1, p. 167, Dec. 2020.
- [9] W. De Schepper, C. Vanschepeael, H. Huynh, and J. Helsen, "Membrane capacitive deionization for cooling water intake reduction in thermal power plants: Lab to pilot scale evaluation," *Energies*, vol. 13, no. 6, p. 1305, Mar. 2020.
- [10] M. Jamróz, M. Piwowarski, P. Ziemiański, and G. Pawlak, "Technical and economic analysis of the supercritical combined gas-steam cycle," *Energies*, vol. 14, no. 11, p. 2985, May 2021.
- [11] G. Mingaleeva, O. Afanaseva, D. T. Nguen, D. N. Pham, and P. Zunino, "The integration of hybrid mini thermal power plants into the energy complex of the republic of Vietnam," *Energies*, vol. 13, no. 21, p. 5848, Nov. 2020.
- [12] J. Liu, Q. Tang, W. Qiu, J. Ma, and J. Duan, "Probability-based failure evaluation for power measuring equipment," *Energies*, vol. 14, no. 12, p. 3632, Jun. 2021.
- [13] D. Singh, V. Kumar, M. Kaur, M. Y. Jabarulla, and H.-N. Lee, "Screening of COVID-19 suspected subjects using multi-crossover genetic algorithm based dense convolutional neural network," *IEEE Access*, vol. 9, pp. 142566–142580, 2021.
- [14] N. Gupta, M. Saini, and A. Kumar, "Operational availability analysis of generators in steam turbine power plants," *SN Appl. Sci.*, vol. 2, no. 4, pp. 1–11, Apr. 2020.

- [15] G. F. M. de Souza, F. J. G. Carazas, L. D. S. Guimarães, and C. E. P. Rodriguez, "Combined-cycle gas and steam turbine power plant reliability analysis," in *Thermal Power Plant Performance Analysis*. London, U.K.: Springer, 2012, pp. 221–247.
- [16] X. Li, N. Wang, L. Wang, I. Kantor, J.-L. Robineau, Y. Yang, and F. Maréchal, "A data-driven model for the air-cooling condenser of thermal power plants based on data reconciliation and support vector regression," *Appl. Thermal Eng.*, vol. 129, pp. 1496–1507, Jan. 2018.
- [17] K. Hooman, "Dry cooling towers as condensers for geothermal power plants," *Int. Commun. Heat Mass Transf.*, vol. 37, no. 9, pp. 1215–1220, Nov. 2010.
- [18] H. Sabouhi, M. Fotuhi-Firuzabad, and P. Dehghanian, "Identifying critical components of combined cycle power plants for implementation of reliability-centered maintenance," *CSEE J. Power Energy Syst.*, vol. 2, no. 2, pp. 87–97, Jun. 2016.
- [19] H. J. Niemann, R. Harte, J. Meyer, and R. Wörmann, "Recent amendments to the VGB Guideline on the design and construction of cooling towers in power plants," *VGB Powertech*, vol. 91, no. 9, p. 94, 2011.
- [20] A. Ayoub, B. Gjorgiev, and G. Sansavini, "Cooling towers performance in a changing climate: Techno-economic modeling and design optimization," *Energy*, vol. 160, pp. 1133–1143, Oct. 2018.
- [21] P. Hartner, J. Petek, P. Pechtl, and P. Hamilton, "Model-based data reconciliation to improve accuracy and reliability of performance evaluation of thermal power plants," in *Proc. Turbo Expo, Power Land, Sea, Air*, vol. 47276, Jan. 2005, pp. 195–200.
- [22] Y. Sun, Z. Guan, and K. Hooman, "A review on the performance evaluation of natural draft dry cooling towers and possible improvements via inlet air spray cooling," *Renew. Sustain. Energy Rev.*, vol. 79, pp. 618–637, Nov. 2017.
- [23] R. Harte, W. B. Krätzig, and H.-J. Niemann, "From cooling towers to chimneys of solar upwind power plants," in *Proc. Struct. Congr., Don't Mess Struct. Eng., Expanding Our Role*, Apr. 2009, pp. 1–10.
- [24] A. S. Stillwell, M. E. Clayton, and M. E. Webber, "Technical analysis of a river basin-based model of advanced power plant cooling technologies for mitigating water management challenges," *Environ. Res. Lett.*, vol. 6, no. 3, Jul. 2011, Art. no. 034015.
- [25] Y. Huang, L. Chen, X. Huang, X. Du, and L. Yang, "Performance of natural draft hybrid cooling system of large scale steam turbine generator unit," *Appl. Thermal Eng.*, vol. 122, pp. 227–244, Jul. 2017.
- [26] P. Reguicki, M. Lewkowicz, R. Krzyżyńska, and H. Jouhara, "Numerical study of water flow rates in power plant cooling systems," *Thermal Sci. Eng. Prog.*, vol. 7, pp. 27–32, Sep. 2018.
- [27] A. E. Conradie and D. G. Kröger, "Performance evaluation of dry-cooling systems for power plant applications," *Appl. Thermal Eng.*, vol. 16, no. 3, pp. 219–232, Mar. 1996.
- [28] H. H. Al-Kayiem and M. A. W. Theeb, "Sustaining thermal power plant production in low water supply regions using cooling towers," *WIT Trans. Ecol. Environ.*, vol. 186, pp. 679–690, Dec. 2014.
- [29] G. R. Biswal, R. P. Maheshwari, and M. L. Dewal, "System reliability and fault tree analysis of SeSHRS-based augmentation of hydrogen: Dedicated for combined cycle power plants," *IEEE Syst. J.*, vol. 6, no. 4, pp. 647–656, Dec. 2012.
- [30] Y. Sun, Z. Guan, H. Gurgenci, J. Wang, P. Dong, and K. Hooman, "Spray cooling system design and optimization for cooling performance enhancement of natural draft dry cooling tower in concentrated solar power plants," *Energy*, vol. 168, pp. 273–284, Feb. 2019.
- [31] L. D. Blackburn, J. F. Tuttle, and K. M. Powell, "Real-time optimization of multi-cell industrial evaporative cooling towers using machine learning and particle swarm optimization," *J. Cleaner Prod.*, vol. 271, Oct. 2020, Art. no. 122175.
- [32] A. Delgado and H. J. Herzog, "Simple model to help understand water use at power plants," Massachusetts Inst. Technol., Cambridge, MA, USA, Tech. Rep., 2012. [Online]. Available: https://energy.mit.edu/wp-content/uploads/2016/12/2012_AD_HJH_WorkingPaper-WaterUse_at_PowerPlants.pdf
- [33] H. Wei, X. Huang, L. Chen, L. Yang, and X. Du, "Performance prediction and cost-effectiveness analysis of a novel natural draft hybrid cooling system for power plants," *Appl. Energy*, vol. 262, Mar. 2020, Art. no. 114555.
- [34] A. H. A. Melani, C. A. Murad, A. C. Netto, G. F. M. Souza, and S. I. Nabeta, "Maintenance strategy optimization of a coal-fired power plant cooling tower through generalized stochastic Petri nets," *Energies*, vol. 12, no. 10, p. 1951, May 2019.
- [35] A. Khodakaram-Tafti and A.-A. Golneshan, "A general mathematical model for predicting the thermal performance of natural draft dry cooling towers and extending it to three aligned towers," *Energy Sources, A, Recovery, Utilization, Environ. Effects*, pp. 1–23, Nov. 2020. [Online]. Available: <https://www.tandfonline.com/doi/full/10.1080/15567036.2020.1844348>
- [36] A. S. Stillwell and M. E. Webber, "Novel methodology for evaluating economic feasibility of low-water cooling technology retrofits at power plants," *Water Policy*, vol. 15, no. 2, pp. 292–308, Apr. 2013.
- [37] F. Khosravi, N. A. Azli, and E. Babaei, "A new modeling method for reliability evaluation of thermal power plants," in *Proc. IEEE Int. Conf. Power Energy*, Nov. 2010, pp. 555–560.
- [38] Q. Han, D. Y. Liu, F. S. Chen, and Z. Yang, "The energy-saving benefit and economic evaluation analysis of cooling tower with flue gas injection," in *Proc. Int. Conf. Sustain. Power Gener. Supply*, Apr. 2009, pp. 1–5.
- [39] T. Wu, Z. Ge, L. Yang, and X. Du, "Modeling the performance of the indirect dry cooling system in a thermal power generating unit under variable ambient conditions," *Energy*, vol. 169, pp. 625–636, Feb. 2019.
- [40] C. C. de França Moraes, P. R. Pinheiro, I. G. Rolim, J. L. de Silva Costa, M. de Silva Elias Junior, and S. J. M. D. Andrade, "Using the multi-criteria model for optimization of operational routes of thermal power plants," *Energies*, vol. 14, no. 12, p. 3682, Jun. 2021, doi: [10.3390/en14123682](https://doi.org/10.3390/en14123682).
- [41] P. Masache, D. Carrión, and J. Cárdenas, "Optimal transmission line switching to improve the reliability of the power system considering AC power flows," *Energies*, vol. 14, no. 11, p. 3281, 2021, doi: [10.3390/en14113281](https://doi.org/10.3390/en14113281).
- [42] F.-S. Kebede, J.-C. Olivier, S. Bourguet, and M. Machmoum, "Reliability evaluation of renewable power systems through distribution network power outage modelling," *Energies*, vol. 14, no. 11, p. 3225, May 2021, doi: [10.3390/en14113225](https://doi.org/10.3390/en14113225).
- [43] R. Benato, A. Chiarelli, and S. D. Sessa, "Reliability assessment of a multi-state HVDC system by combining Markov and matrix-based methods," *Energies*, vol. 14, no. 11, p. 3097, May 2021, doi: [10.3390/en14113097](https://doi.org/10.3390/en14113097).
- [44] H. Seyedhashemi, B. Hingray, C. Lavaysse, and T. Chamarande, "The impact of low-resource periods on the reliability of wind power systems for rural electrification in Africa," *Energies*, vol. 14, no. 11, p. 2978, May 2021, doi: [10.3390/en14112978](https://doi.org/10.3390/en14112978).
- [45] R. Sun, G. Abeynayake, J. Liang, and K. Wang, "Reliability and economic evaluation of offshore wind power DC collection systems," *Energies*, vol. 14, no. 10, p. 2922, May 2021, doi: [10.3390/en14102922](https://doi.org/10.3390/en14102922).
- [46] H. Zhang, "Transient performance of the particle swarm optimization algorithm from system dynamics point of view," *J. Comput. Inf. Sci. Eng.*, vol. 20, no. 4, 2020, Art. no. 041008.
- [47] J. Li, Z. Liu, and X. Wang, "Public charging station location determination for electric ride-hailing vehicles based on an improved genetic algorithm," *Sustain. Cities Soc.*, vol. 74, Nov. 2021, Art. no. 103181.
- [48] G.-G. Wang, A. H. Gandomi, A. H. Alavi, and S. Deb, "A hybrid method based on krill herd and quantum-behaved particle swarm optimization," *Neural Comput. Appl.*, vol. 27, no. 4, pp. 989–1006, May 2016, doi: [10.1007/s00521-015-1914-z](https://doi.org/10.1007/s00521-015-1914-z).
- [49] H. P. Jagtap, A. K. Bewoor, R. Kumar, M. H. Ahmadi, and L. Chen, "Performance analysis and availability optimization to improve maintenance schedule for the turbo-generator subsystem of a thermal power plant using particle swarm optimization," *Rel. Eng. Syst. Saf.*, vol. 204, Dec. 2020, Art. no. 107130.
- [50] J. H. Holland, "Genetic algorithms," *Sci. Amer.*, vol. 267, no. 1, pp. 66–73, 1992.
- [51] D. E. Goldberg and J. H. Holland, "Genetic algorithms and machine learning," *Mach. Learn.*, vol. 3, nos. 2–3, pp. 95–99, 1988.
- [52] R. Eberhart and J. Kennedy, "A new optimizer using particle swarm theory," in *Proc. 6th Int. Symp. Micro Mach. Human Sci.*, Oct. 1995, pp. 39–43.
- [53] S. Mirjalili, S. M. Mirjalili, and A. Lewis, "Grey wolf optimizer," *Adv. Eng. Softw.*, vol. 69, pp. 46–61, Mar. 2014.
- [54] M. Dorigo, M. Birattari, and T. Stutzle, "Ant colony optimization," *IEEE Comput. Intell. Mag.*, vol. 1, no. 4, pp. 28–39, Nov. 2006.
- [55] G. Wang, S. Deb, and Z. Cui, "Monarch butterfly optimization," *Neural Comput. Appl.*, vol. 31, no. 7, pp. 1995–2014, Jul. 2019.
- [56] G.-G. Wang, S. Deb, and L. D. S. Coelho, "Earthworm optimisation algorithm: A bio-inspired metaheuristic algorithm for global optimisation problems," *Int. J. Bio-Inspired Comput.*, vol. 12, no. 1, pp. 1–22, Jan. 2018.
- [57] G.-G. Wang, S. Deb, and L. D. S. Coelho, "Elephant herding optimization," in *Proc. 3rd Int. Symp. Comput. Bus. Intell. (ISCBI)*, Dec. 2015, pp. 1–5.
- [58] G. G. Wang, "Moth search algorithm: A bio-inspired metaheuristic algorithm for global optimization problems," *Memetic Comput.*, vol. 10, no. 2, pp. 151–164, Jun. 2016.

- [59] S. Li, H. Chen, M. Wang, A. A. Heidari, and S. Mirjalili, "Slime mould algorithm: A new method for stochastic optimization," *Future Gener. Comput. Syst.*, vol. 111, pp. 300–323, Oct. 2020.
- [60] A. A. Heidari, S. Mirjalili, H. Faris, I. Aljarah, M. Mafarja, and H. Chen, "Harris hawks optimization: Algorithm and applications," *Future Gener. Comput. Syst.*, vol. 97, pp. 849–872, Aug. 2019.
- [61] J. Derrac, S. García, D. Molina, and F. Herrera, "A practical tutorial on the use of nonparametric statistical tests as a methodology for comparing evolutionary and swarm intelligence algorithms," *Swarm Evol. Comput.*, vol. 1, no. 1, pp. 3–18, Mar. 2011.
- [62] R. Storn and K. Price, "Differential evolution—A simple and efficient heuristic for global optimization over continuous spaces," *J. Global Optim.*, vol. 11, no. 4, pp. 341–359, 1997.
- [63] M. Kaur and D. Singh, "Multiobjective evolutionary optimization techniques based hyperchaotic map and their applications in image encryption," *Multidimensional Syst. Signal Process.*, vol. 32, no. 1, pp. 281–301, Jan. 2021.
- [64] M. Baiocchi, A. Milani, and V. Santucci, "Variable neighborhood algebraic differential evolution: An application to the linear ordering problem with cumulative costs," *Inf. Sci.*, vol. 507, pp. 37–52, Jan. 2020.
- [65] V. Santucci, A. Milani, and F. Caraffini, "An optimisation-driven prediction method for automated diagnosis and prognosis," *Mathematics*, vol. 7, no. 11, p. 1051, Nov. 2019.
- [66] M. Kaur, V. Kumar, V. Yadav, D. Singh, N. Kumar, and N. N. Das, "Metaheuristic-based deep COVID-19 screening model from chest X-ray images," *J. Healthcare Eng.*, vol. 2021, pp. 1–9, Mar. 2021, doi: [10.1155/2021/8829829](https://doi.org/10.1155/2021/8829829).
- [67] M. Saini and A. Kumar, "Stochastic modeling of a single-unit system operating under different environmental conditions subject to inspection and degradation," *Proc. Nat. Acad. Sci., India Sect. A, Phys. Sci.*, vol. 90, no. 2, pp. 319–326, Jun. 2020.
- [68] M. Khishe and M. R. Mosavi, "Chimp optimization algorithm," *Expert Syst. Appl.*, vol. 149, Jul. 2020, Art. no. 113338.
- [69] M. Khishe, M. Nezhadshahbodaghi, M. R. Mosavi, and D. Martin, "A weighted chimp optimization algorithm," *IEEE Access*, vol. 9, pp. 158508–158539, 2021.
- [70] M. Khishe, M. R. Mosavi, and M. Kaveh, "Improved migration models of biogeography-based optimization for sonar dataset classification by using neural network," *Appl. Acoust.*, vol. 118, pp. 15–29, Mar. 2017.
- [71] W. Kaidi, M. Khishe, and M. Mohammadi, "Dynamic Levy flight chimp optimization," *Knowl.-Based Syst.*, vol. 235, Jan. 2022, Art. no. 107625.
- [72] J. Wang, M. Khishe, M. Kaveh, and H. Mohammadi, "Binary chimp optimization algorithm (BChOA): A new binary meta-heuristic for solving optimization problems," *Cognit. Comput.*, vol. 13, no. 5, pp. 1297–1316, Sep. 2021.
- [73] D. Jiang, G. Hu, G. Qi, and N. Mazur, "A fully convolutional neural network-based regression approach for effective chemical composition analysis using near-infrared spectroscopy in cloud," *J. Artif. Intell. Technol.*, vol. 1, no. 1, pp. 74–82, Jan. 2021.
- [74] H. S. Basavegowda and G. Dagnev, "Deep learning approach for microarray cancer data classification," *CAAI Trans. Intell. Technol.*, vol. 5, no. 1, pp. 22–33, Mar. 2020.
- [75] Y. Xu and T. T. Qiu, "Human activity recognition and embedded application based on convolutional neural network," *J. Artif. Intell. Technol.*, vol. 1, no. 1, pp. 51–60, Dec. 2020.
- [76] S. Ghosh, P. Shivakumara, P. Roy, U. Pal, and T. Lu, "Graphology based handwritten character analysis for human behaviour identification," *CAAI Trans. Intell. Technol.*, vol. 5, no. 1, pp. 55–65, Mar. 2020.
- [77] G. Hu, S.-H. K. Chen, and N. Mazur, "Deep neural network-based speaker-aware information logging for augmentative and alternative communication," *J. Artif. Intell. Technol.*, vol. 1, no. 2, pp. 138–143, 2021.
- [78] B. Gupta, M. Tiwari, and S. S. Lamba, "Visibility improvement and mass segmentation of mammogram images using quantile separated histogram equalisation with local contrast enhancement," *CAAI Trans. Intell. Technol.*, vol. 4, no. 2, pp. 73–79, Jun. 2019.
- [79] V. V. Singh, M. Ram, and D. K. Rawal, "Cost analysis of an engineering system involving subsystems in series configuration," *IEEE Trans. Autom. Sci. Eng.*, vol. 10, no. 4, pp. 1124–1130, Oct. 2013.
- [80] M. Ram, S. B. Singh, and V. V. Singh, "Stochastic analysis of a standby system with waiting repair strategy," *IEEE Trans. Syst., Man, Cybern., Syst.*, vol. 43, no. 3, pp. 698–707, May 2013.
- [81] A. Sharma, A. Sharma, A. Dasgotra, V. Jatley, M. Ram, S. Rajput, M. Averbukh, and B. Azzopardi, "Opposition-based tunicate swarm algorithm for parameter optimization of solar cells," *IEEE Access*, vol. 9, pp. 125590–125602, 2021.



ASHISH KUMAR received the M.Sc., M.Phil., and Ph.D. degrees in 2009, 2010, and 2013, respectively. He is currently working with the Department of Mathematics and Statistics, Manipal University Jaipur, Jaipur, India, as an Assistant Professor. His research interests include reliability modeling, reliability estimation, and sampling theory.



MONIKA SAINI received the M.Sc., M.Phil., and Ph.D. degrees in 2008, 2009, and 2012, respectively. She is currently working with the Department of Mathematics and Statistics, Manipal University Jaipur, Jaipur, India, as an Assistant Professor. Her research interests include reliability modeling, reliability estimation, and sampling theory.



NIVEDITA GUPTA received the M.Sc. degree in statistics from Rajasthan University. She is currently doing her research work at the Department of Mathematics and Statistics, Manipal University Jaipur, Jaipur, India. Her research interests include reliability modeling and analysis.



DEEPAK SINWAR (Member, IEEE) received the Bachelor of Technology degree in information technology, in 2008, and the Master of Technology and Ph.D. degrees in computer science and engineering, in 2010 and 2016, respectively. He is currently an Assistant Professor with the Department of Computer and Communication Engineering, School of Computing and Information Technology, Manipal University Jaipur, Jaipur, Rajasthan, India. He is an enthusiastic and motivating technocrat with more than 11 years of research and academic experience at different institutes. His research interests include computational intelligence, data mining, machine learning, reliability theory, computer networks, and pattern recognition. He is a Life Member of ISTE (India) and a member of ACM.



DILBAG SINGH (Member, IEEE) received the M.Tech. degree from the Computer Science and Engineering Department, Guru Nanak Dev University, India, in 2012, and the Ph.D. degree in computer science and engineering from Thapar University, India, in 2019. He is currently working as a Research Professor with the School of Electrical Engineering and Computer Science, GIST, South Korea. He has helped many under-graduate students to successfully implement their project work. He is the author or coauthor of more than 70 SCI/SCIE indexed journals, including refereed IEEE/ACM/Springer/Elsevier journals. He has also obtained three patents, three books, and two book chapters. His research interests include computer vision, medical image processing, machine learning, deep learning, information security, and meta-heuristic techniques. He was in the Top 2% list issued by the World Ranking of Top 2% Scientists in 2021. He was a part of the 11 Web of Science/Scopus indexed conferences. He is also acting as a Lead Guest Editor of *Mathematical Problems in Engineering* (Hindawi, SCI and Scopus Indexed), an Executive Guest Editor of *Current Medical Imaging* (Bentham Science, SCIE and Scopus Indexed), and an Associate Editor of *Open Transportation Journal* (Scopus). He is a Reviewer of more than 60 well-reputed journals, such as IEEE, Elsevier, Springer, SPIE, and Taylor and Francis.



MANJIT KAUR (Member, IEEE) received the Ph.D. degree in image processing from the Thapar Institute of Engineering and Technology, Patiala, Punjab, India, and the Master of Engineering degree in information technology from Panjab University, Chandigarh, Punjab, India. She is currently working as a Postdoctoral Researcher with the School of Electrical Engineering and Computer Science, GIST, South Korea. She has published more than 60 SCI/SCIE indexed articles so far. Her research interests include wireless sensor networks, digital image processing, and meta-heuristic techniques.



HEUNG-NO LEE (Senior Member, IEEE) received the B.S., M.S., and Ph.D. degrees in electrical engineering from the University of California at Los Angeles, CA, USA, in 1993, 1994, and 1999, respectively. He was with HRL Laboratories, LLC, Malibu, CA, USA, as a Research Staff Member, from 1999 to 2002. From 2002 to 2008, he was an Assistant Professor with the University of Pittsburgh, PA, USA. In 2009, he moved to the School of Electrical Engineering and Computer Science, Gwangju Institute of Science and Technology, Gwangju, South Korea, where he is currently affiliated. His research interests include information theory, signal processing theory, blockchain, communications/networking theory and their application to wireless communications and networking, compressive sensing, future internet, and brain-computer interface. He has received several prestigious national awards, including the Top 100 National Research and Development Award in 2012, the Top 50 Achievements of Fundamental Researches Award in 2013, and the Science/Engineer of the Month in January 2014.

• • •